Journal of Aerosol Science 57 (2013) 156–178

Contents lists available at SciVerse ScienceDirect

Journal of Aerosol Science

journal homepage: www.elsevier.com/locate/jaerosci

Comparability of mobility particle sizers and diffusion chargers

Heinz Kaminski [a], Thomas A.J. Kuhlbusch [a,f], Stefan Rath [b], Uwe Götz [b], Manfred Sprenger [b], Detlef Wels [b], Jens Polloczek [b], Volker Bachmann [c], Nico Dziurowitz [c], Heinz-Jürgen Kiesling [d], Angelika Schwiegelshohn [d], Christian Monz [e], Dirk Dahmann [e], Christof Asbach [a,*]

[a] Institute of Energy and Environmental Technology (IUTA) e.V., Air Quality & Sustainable Nanotechnology unit, Bliersheimer Str. 60, Germany
[b] BASF SE, 67063 Ludwigshafen, Germany
[c] Federal Institute of Occupational Safety and Health (BAuA), Nöldnerstr. 40–42, 10317 Berlin, Germany
[d] Bayer Technology Services GmbH, 51368 Leverkusen, Germany
[e] Institute for the Research on Hazardous Substances (IGF), Waldring 97, 44789 Bochum, Germany
[f] Center for NanoIntegration Duisburg-Essen (CENIDE), 47057 Duisburg, Germany

ARTICLE INFO

Article history:
Received 25 July 2012
Received in revised form
4 October 2012
Accepted 15 October 2012
Available online 15 November 2012

Keywords:
SMPS
FMPS
Diffusion charger
CPC
Electrical mobility analysis

ABSTRACT

A large study on the comparability of various aerosol instruments was conducted. The study involved altogether 24 instruments, including eleven scanning, sequential and fast mobility particle sizers (five Grimm SMPS+C, three TSI SMPS and three FMPS) with different settings and differential mobility analyzers (DMAs), twelve instruments based on unipolar diffusion charging to determine size integrated concentrations and in some cases mean particle size (five miniDiSCs of the University of Applied Sciences and Arts Northwestern Switzerland, four Philips Aerasense nanoTracers, two TSI Nanoparticle Surface Area Monitors and one Grimm nanoCheck) and one TSI ultrafine condensation particle counter (UCPC). All instruments were simultaneously challenged with particles of various sizes, concentrations and morphologies. All measurement results were compared with those from a freshly calibrated SMPS for size distributions and the UCPC for number concentration. In general, all SMPSs showed good comparability with particularly the sizing agreeing to within a few percent. Differences in the determined number concentration were somewhat more pronounced, but the largest deviations could be tracked back to the use of an older software version. The comparability of the FMPSs was shown to be lower, with discrepancies on the order of $\pm 25\%$ for sizing and $\pm 30\%$ for total concentrations. The discrepancies between FMPSs and the internal reference SMPS seemed to be influenced by particle size and morphology. Total number and/or lung deposited surface area concentrations measured with unipolar diffusion charger based instruments generally agreed to within $\pm 30\%$ with the internal references (CPC for number concentrations; lung deposited surface area derived from SMPS measurements), as long as the particle size distributions of the test aerosols were within the specified limits for the instruments. When the upper size limit was exceeded, deviations of up to several hundred percent were detected.

* Corresponding author. Tel.: +49 2065 418 209; fax: +49 2065 418 211.
E-mail address: asbach@iuta.de (C. Asbach).

0021-8502/$ - see front matter © 2012 Elsevier Ltd. All rights reserved.
http://dx.doi.org/10.1016/j.jaerosci.2012.10.008

1. Introduction

Aerosol instruments are used in a wide range of applications, e.g., in ambient air quality or exhaust gas monitoring, (workplace) exposure assessment or process control due to possible negative effects of aerosols onto humans, the environment or products. Traditionally, particles in an aerosol are quantified by means of mass concentrations, often as size-limited sub-fractions such as PM_{10} or $PM_{2.5}$ in the case of ambient air or as the respirable or inhalable particle size fraction (according to DIN EN 481) in the case of workplace exposure studies. However, several studies have shown that potential adverse health effects may increase with decreasing particle size (e.g., Peters et al., 1997; Oberdörster et al., 2005; Oberdörster, 2001), which shifted the focus more towards ultrafine or nanoparticles[1] (both <100 nm). Since the particle mass scales with the third power of the particle diameter, nanoscale particles usually contribute only negligibly to total mass concentrations. The measurement of particle number rather than mass is therefore commonly preferred. For example the Euro 6 standard sets limits for the total number of particles emitted from light passenger and commercial vehicles (European Parliament and the Council, 2007). Several studies have been carried out to determine the number concentration and size distribution in ambient air (Shi et al., 1999; Buzorius et al., 1999; Kuhlbusch et al., 2001; Wehner et al., 2002). With the increasing production of engineered nanoparticles, not only process control measurements have shifted towards the determination of particle number concentrations and size distributions, but also occupational exposure assessment in workplaces, where nanoparticles are produced, handled or used otherwise. Most studies on exposure to engineered nanoparticles that have been published in the recent years focused on the measurement of particle number concentration or particle number size distributions (Brouwer et al., 2009; Kuhlbusch et al., 2011).

Besides the particle number concentration, particle surface area concentration has been proposed as a more health relevant aerosol metric (Oberdörster, 2000), because the particle surface area is the interface between the particle and the lung upon inhalation. Several toxicological studies have shown that adverse health effects showed the best correlation with the particle surface area dose, rather than the particle number or mass doses (Oberdörster, 2000; Duffin et al., 2002; Tran et al., 2000).

A variety of instruments have been developed over the past decades to quantify airborne particles in the submicron size range. These include condensation particle counters (CPC) for the measurement of size-integrated particle number concentrations and electrical mobility spectrometers such as scanning or sequential mobility particle sizer (SMPS, Wang & Flagan, 1990) and fast mobility particle sizer (FMPS, Tammet et al., 2002) for the measurement of particle number size distributions. In addition, instruments based on electrical diffusion charging have emerged over the recent years that are capable of measuring the total particle number concentration, usually along with the mean particle diameter, and/or the fraction of the airborne particle surface area concentration that would deposit in the human respiratory tract.

Determination of the comparability and reproducibility of the abovementioned instruments is crucial in view of comparability of measurement results obtained with several specimens of the same instrument type or in view of potential future legislative limit values. While the accuracy of particle sizing can fairly easily be assessed by dispersing polystyrene latex spheres of well known sizes, a calibration check for the particle number concentration is usually not possible for end users, due to the lack of a "standard aerosol". Although several studies have been published that present generators for reference aerosols with predictable particle number concentrations (Koch et al., 2008; Yli-Ojanpera et al., 2010), these generators are not commercialized and hence usually not available for instrument calibration. The lack of knowledge on the "true" particle number or surface area concentration in an aerosol makes intercomparison of the instruments the only feasible way for assessing the comparability of devices. We here present an intensive study on the comparability of a large variety of instruments, measuring particle number size distributions, particle number concentrations and lung deposited surface area concentrations. The aim of the study was to compare the response of the instruments to various aerosols, concerning the particle sizes, concentrations and particle morphologies.

2. Methods

2.1. Experimental set up

Experiments were conducted at the NanoTestCenter of the Institute for the Research on Hazardous Substances (IGF) in Dortmund, Germany. The set up is based on an earlier test stand for the generation of diesel soot test particles (Dahmann, 1997). The measurement facility is specifically designed for the comparison of aerosol measurement devices with well defined aerosols. A schematic of the set up is shown in Fig. 1. Four different types of aerosol generators can be used: (1) a home-made atomizer to produce particles from a solution (e.g., Sodium Chloride, NaCl), suspension (e.g., Polystyrene Latex spheres, PSL) or to produce small droplets of a liquid with high surface tension (e.g., Di-Ethyl-Hexyl-Sebacate, DEHS, $C_{26}H_{50}O_4$); (2) a spark generator (Palas GFG3000) to produce agglomerated particles, typically carbon-aerosol ("soot") from graphite electrodes, but metal and metal-oxide particles are also possible; (3) a home-built flame generator to produce metal oxide particles; and (4) a diesel engine (aspiration type, 2180 cm^3, Mercedes Benz 220D, 44 kW at

[1] Ultrafine particles denote all intentionally and unintentionally produced particles, single or agglomerated, with at least one dimension <100 nm. Nanoparticles denote only the intentionally produced particles within this size class range.

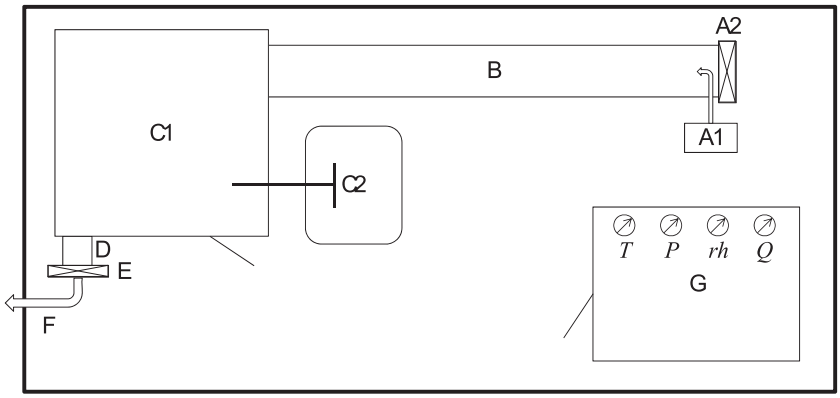

A1 Aerosol generation (atomizer, spark generator or flame generator), drying and neutralization
A2 Optional ULPA background filter
B Wind tunnel, approximately 20 m long, 0.7 m diameter
C1 Measurement chamber, approximately 20 m³
C2 T-shaped sampling train
D Blower
E Exhaust filter
F Exhaust
G Control room for flow rate *Q*, measurement of temperature *T*, pressure *P* and relative humidity *rh* in measurement chamber C1

Fig. 1. Experimental set up in the NanoTestCenter; during measurements, all FMPSs, miniDiSCs, nanoTracers, nanoCheck, NSAMs as well as the internal reference CPC and SMPS-G1 were located inside the measurement chamber (C1), all other SMPSs were located outside the chamber and sampled via the T-shaped sampling train (C2).

4200 rpm) to produce agglomerated diesel soot particles. The prior two generators were used in this comparison study. They as well as the flame generator allow for the control or the variation within certain limits of the particle size through the amount of material in suspension/solution (atomizer), the total current, inert gas and dilution air flow (spark generator) and the amount and material of the precursor (flame generator). While the atomizer is usually used to produce compact particles, i.e., cubic in the case of NaCl and spherical in the case of DEHS, the spark and flame generators produce very high concentrations of small primary particles that quickly coagulate to form agglomerates or aggregates. The degree of agglomeration can best be controlled with the spark generator by the amount of dilution air that is introduced into the device. The size and shape of the particles furthermore depends on the material used. The freshly produced particles are neutralized with an ^{85}Kr Neutralizer (TSI, model 3012A; 370 MBq initial activity) immediately downstream of the particle generators (see Fig. 1) and, in the case of atomized suspensions or solutions, additionally dried in a home-made coaxial silica gel dryer.

The generated aerosol is then introduced into an approximately 20 m long wind tunnel with 70 cm diameter where it is mixed with ULPA (ultra-low penetration air)-filtered dilution air. The amount of dilution air can be adjusted to control the particle concentration. The wind tunnel is long enough to assure perfect mixing of the generated aerosol with the dilution air. The wind tunnel feeds into a closed mixing chamber with a volume of approximately 20 m^3. The air flow through the chamber and the wind tunnel is provided by a blower outside the mixing chamber. It was previously shown that the aerosol is homogenously distributed throughout the mixing chamber, such that all instruments can be placed inside the chamber to sample the same aerosol. The concentration may only differ near the chamber walls (Asbach et al., 2012). The chamber is sufficiently large to simultaneously host dozens of instruments ensuring the sampling of the identical aerosol. Those instruments that require frequent attention or adjustment can be placed outside the chamber and connected to a sampling train that withdraws aerosol from within the chamber. The sampling train is T-shaped and has connections for up to six instruments on each end of the T (see Fig. 1). It has been shown in numerous previous studies (unpublished) that the submicron size distributions measured downstream of the sampling train are identical with those inside the chamber, except for diffusion losses. Diffusion losses in the sampling train were kept low by maintaining a flow rate of 20 lpm in the first and 10 lpm in the two distributing legs of the sampling train. The losses were calculated according to equations in Hinds' (1999) textbook and found to be on the order of only a few percent even for the smallest particles (NaCl) used in this study. Diffusion losses in the sampling train were therefore neglected here. The NanoTestCenter has successfully been used for several intercomparison studies in the past (Asbach et al., 2009a, 2012; Dahmann et al., 2001).

In the present study, NaCl and DEHS particles were produced with the atomizer and soot particles with the spark generator. These materials were chosen to allow coverage of a large range of particle sizes and morphologies. While atomized DEHS forms spherical droplets, NaCl particles are known to be cubic, i.e., close to spherical. To the contrary, the soot (carbon) particles from the spark generator were elongated agglomerates of smaller spherical primary particles (Fig. 2).

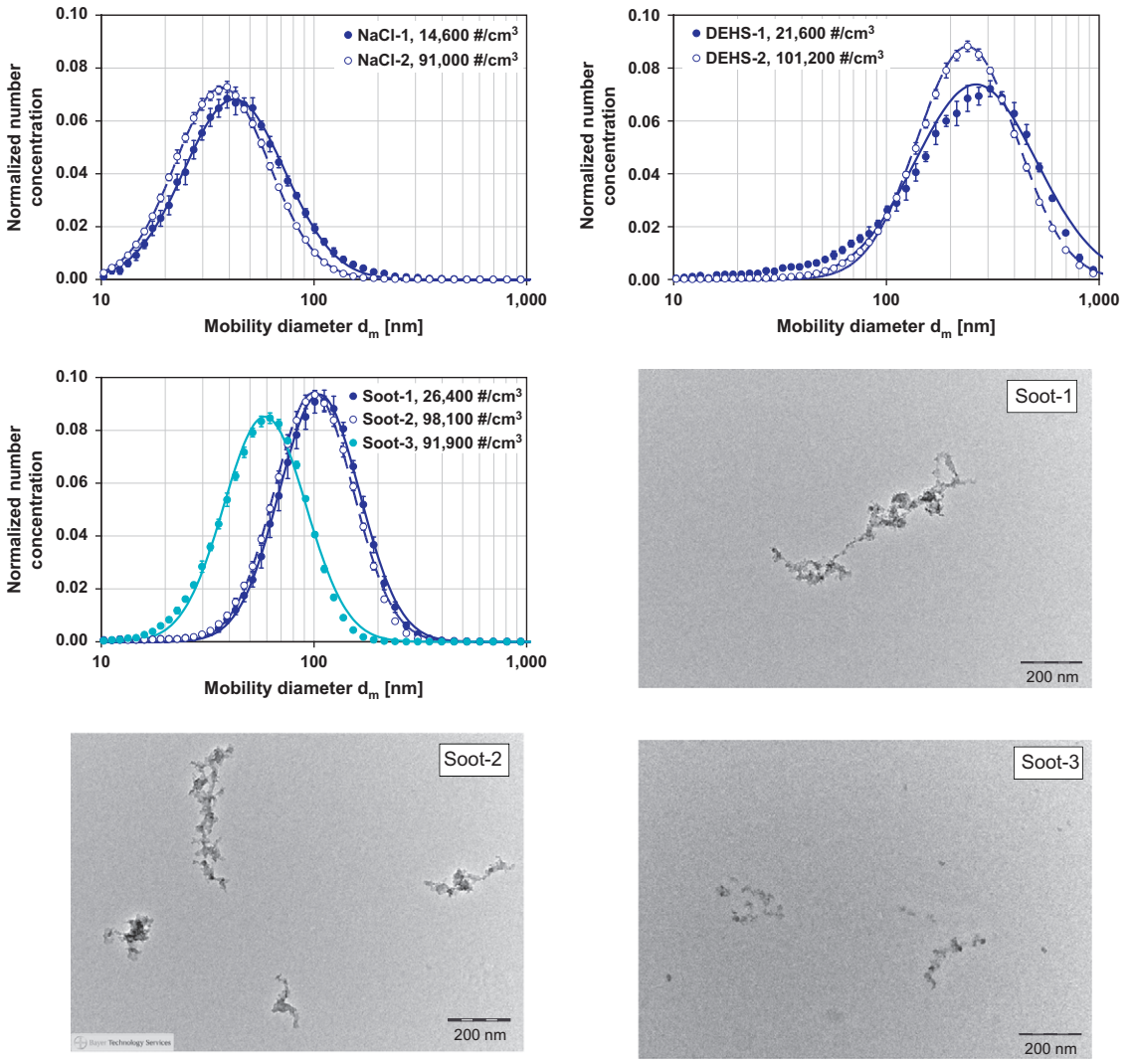

Fig. 2. Normalized size distributions of the test aerosols; top left: NaCl, top right: DEHS, center left: soot, measured with the SMPS-G1, symbols are measurement data, error bars indicate the standard deviation, lines are lognormal fitted data; the TEM images (magnification 100,000:1) shows a typical soot test particle for soot-1, soot-2 and soot-3 from the spark generator.

One Scanning Mobility Particle Sizer (SMPS+C, Grimm Aerosoltechnik, Germany) was freshly calibrated by the manufacturer and served as an internal reference, in this study named as SMPS-G1. In addition, a stand-alone butanol Ultrafine Condensation Particle Counter (UCPC, TSI model 3776, size range 2.5 nm to several μm) was used to monitor the total particle number concentration and its stability. This particular model can measure up to 3×10^5 #/cm^3 in single particle count mode. After switching a particle generator on it usually took 5–10 min for the total concentration in the chamber to stabilize. The number concentration then remained constant for up to several hours with deviations of usually less than $\pm5\%$. Measurements were hence started approximately 15 min after a generator was switched on. Normalized size distributions of the test aerosols, measured with the SMPS-G1 are shown in Fig. 2 along with TEM images of typical soot test particles from the spark generator. Particles for TEM analysis were sampled with a Nanometer Aerosol Sampler (TSI, model 3089; Dixkens & Fissan, 1999). The NAS was used without an upstream charger and hence sampling at a relatively low efficiency, relying only on the "natural" charge of the particles. This was done in order not to overload the TEM grids to avoid overlapping particles on the grid. Particles were sampled for 30 min at a flow rate of 1.5 lpm and a collection voltage of +10 kV. The mean charge level of the test aerosol in the mixing chamber was continuously monitored with an aerosol electrometer (TSI, model 3068B). Average charge levels were slightly negative, but found to be well below one elementary charge per particle (results not shown here), indicating the effective neutralization of the aerosol downstream of the generator. Each size distribution in Fig. 2 represents the average of a one hour measurement. Error bars indicate the standard deviation of the measured concentrations in each size bin. For better clarity of representation, the size distributions are normalized with respect to the integral of the $dN/d\log(d_p)$ distribution, such that the integral of each

Table 1
Overview of mobility spectrometers and their settings in this study.

Manufacturer & model no.	Instrument ID	DMA	Size range (nm)	Size resolution	Time resolution (s)	Aerosol/sheath flow (lpm)	Software version
Grimm, SMPS+C	SMPS-G1, SMPS-G2	L-DMA	10.3–1091		415	0.3/3	5.477, vers. 1.2.1
	SMPS-G3, SMPS-G4	L-DMA	11.1–1083	45 channels (total)	406	0.3/3	5.477, vers. 1.34
	SMPS-G5	M-DMA	5.5–350		230	0.3/3	5.477, vers. 1.34
TSI SMPS, model 3936	SMPS-T1[a]	TSI-long	9.7–421	64 ch./decade	300	0.6/6	AIM, vers. 9.0.0.1
	SMPS-T2[b], SMPS-T3[c]	TSI-long	13.8–750		300	0.3/3	AIM, vers. 8.1.0.0
TSI FMPS, model 3091	FMPS-1 to FMPS-3		5.6–560	16 ch./decade	1	10/40	vers. 2.1.2.0

[a] With CPC 3010.
[b] With UWCPC 3786.
[c] With UCPC 3776.

normalized size distribution is one. The total number concentrations are given in the legend of each graph. The particle concentrations were adjusted to two levels for each particle material by changing the dilution air flow rate in the wind tunnel, one around 20,000 #/cm^3 and the other one around 100,000 #/cm^3. This was done to investigate a possible effect of particle concentration on the particle measurement. However, both concentrations are well within the concentration ranges of all instruments in the study. Fig. 2 shows that the dilution in the wind tunnel mainly affected the concentrations and had only a minor impact on the particle size distributions. Since the soot particle morphology deviated most from the commonly assumed spherical particle shape, two different settings of the spark generator were tested that produced different size distributions (see lower left graph Fig. 2). The soot-1 and soot-2 setting was chosen such that the entire size distribution (modal diameter around 100 nm, geometric standard deviation of 1.54) is well within the size limits of all instruments in the test, whereas the size distribution of soot-3 contains particles in the area of and below the lower size limit of some diffusion charger based instruments in the study. Still, the size range of soot-3 was in the range of the electrical mobility spectrometers. This setting thus allowed for the study of possible size-dependent morphology effects on electrical mobility analysis while at the same time possible effects of the lower detection limit of diffusion chargers could be studied.

2.2. Instrumentation

2.2.1. Instruments measuring particle size distributions

Instruments for measuring particle size distributions were all based on electrical mobility analysis. They are summarized in Table 1. The different settings of the mobility spectrometers represent the typical settings used by the respective partner and were chosen to cover a wide range of possible instrument settings. The equipment included scanning mobility particle sizers from two manufacturers (SMPS+C, Grimm Aerosoltechnik, Ainring, Germany and SMPS 3936, TSI Inc, Shoreview, MN, USA) as well as Fast Mobility Particle Sizers (FMPS, TSI model 3091). It should be noted that the SMPSs from the two manufacturers use slightly different principles. While a TSI SMPS continuously ramps the DMA voltage and is hence a true Scanning Mobility Particle Sizers (Wang and Flagan, 1990), a Grimm SMPS sequentially applies the DMA voltages in steps, similar to a Differential Mobility Particle Sizer (DMPS; Hoppel, 1978; Fissan et al., 1983). However, since both manufacturers call their instruments Scanning Mobility Particle Sizer, this term is used here synonymously for both principles. Altogether five Grimm SMPSs were used. They differed in the length of the Vienna-type differential mobility analyzers (Winklmayr et al., 1991) and the software versions used for data acquisition and evaluation. All Grimm SMPSs used the standard Grimm ^{241}Am neutralizer (model 5.521) with an initial activity of 3.7 MBq. SMPS-G1 and SMPS-G2 were both equipped with a long DMA (L-DMA, model 55-900) and the newest software version (version 1.2.1). SMPS-G3 and SMPS-G4 also used the same type of long DMA, but an older software version (5.477, version 1.34). SMPS-G5 used the same older software version, but a short DMA (M-DMA, model 55-340). With these configurations, SMPS-G1 and SMPS-G2 measured particle number size distributions in a size range from 10.3 to 1091 nm with 415 s time resolution and provided the size distributions in a total of 45 channels. SMPS-G3 and SMPS-G4 measured particle number size distribution in a size range from 11.1 to 1083 nm with 406 s time resolution in a total of 44 channels. SMPS-G5 was configured to measure size distributions in a range from 5.5 to 350 nm with 230 s time resolution in a total of 44 channels. All Grimm SMPSs were used with identical Condensation Particle Counters (Grimm, model 5.403). Correction for diffusional losses in the SMPS is inherently included in the Grimm SMPS software.

A total of three TSI SMPSs (model 3936) were involved in the study that differed in the flow rate settings as well as in the employed CPCs. All TSI SMPSs were equipped with a long DMA (model 3081, Pui & Liu, 1974). SMPS-T1 measured with 0.6 lpm aerosol flow and 6 lpm sheath flow rate and used a butanol CPC (TSI model 3010). SMPS-T2 and SMPS-T3 used 0.3 lpm aerosol and 3 lpm sheath flow rate. SMPS-T2 was equipped with an ultrafine water CPC (TSI, model 3786) and SMPS-T3 with an ultrafine butanol CPC (TSI, model 3776). SMPS-T1 and SMPS-T2 used a ^{85}Kr neutralizer with an initial activity of 74 MBq (TSI, model 3077), whereas SMPS-T3 used a 370 MBq ^{85}Kr neutralizer (TSI, model 3077A). All three TSI SMPSs were set to 240 s scan and 20 s retrace time. Another 40 s were waited before a new scan was started, resulting in

an overall time resolution of 300 s. All TSI SMPSs were operated using Aerosol Instrument Manager software (SMPS-T1 with version 9.0.0.1, SMPS-T2 and SMPS-T3 with version 8.1.0.0) and delivered size distributions in a size range from 9.7 nm to 421 nm (SMPS-T1) and from 13.8 nm to 750 nm (SMPS-T2 and SMPS-T3) with a size resolution of 64 channels per size decade. Correction for diffusional particle losses was enabled for all TSI SMPSs.

Three identical Fast Mobility Particle Sizers (FMPS, TSI model 3091) were used. Unlike the SMPS, the FMPS uses a unipolar corona charger and measures the different particle mobilities simultaneously by using an array of 22 electrometers along the outer classifier electrode. The measured mobility-current distribution is deconvoluted into a number size distribution in a size range from 5.6 nm to 560 nm, which is reported with 1 s time resolution in 16 channels per size decade. Diffusion losses in the FMPS are unknown and could hence not be corrected. However, due to its high flow rates (10 lpm aerosol and 40 lpm sheath flow) diffusion losses are assumed to be very low in the FMPS.

Prior to the intercomparison measurements, the calibration for the sizing of all SMPSs in the study has been checked by dispersing suspensions of monodisperse PSL particles (BS-Partikel, Wiesbaden, Germany) with an atomizer (model ATM 226, TOPAS GmbH, Dresden, Germany). Two different PSL particle sizes were used, 95.6 ± 1.2 nm and 246 ± 6 nm. Since the exact sizes of the PSL particles do not match the center points of the SMPS size channels, the measured size distributions of the singlet particles were fitted to lognormal distributions to determine their modal diameters and geometric standard deviations. The agreement of the reported modal diameters with the nominal diameters of the PSL particles was very good. For 95.6 nm PSL particles, the SMPSs measured modal diameters between 94.9 nm (SMPS-G5) and 99.5 nm (SMPS-G4). The reported modal diameters for 246 nm PSL particles were between 247.1 nm (SMPS-T2) and 258.4 nm (SMPS-G3). The observed small deviations from the nominal PSL sizes were random and could not be linked to a particular manufacturer or model. The calibration of the FMPS could not be checked, because its algorithm does not allow for meaningful measurements of monodisperse particles (Leskinen et al., 2012).

2.2.2. *Instruments measuring size-integrated concentrations*

Several instruments were used in the study to measure total size integrated number or lung deposited surface area concentrations. They are summarized in Table 2. A butanol-based ultrafine condensation particle counter (TSI, model 3776) was used as an internal reference for the number concentration. According to the manufacturer's specifications, this CPC covers the size range between 2.5 nm and a few microns and uses the very accurate single particle counting mode up to a concentration of 300,000 #/cm^3. In addition four different types of instruments were used that are based on electrical unipolar diffusion charging followed by the measurement of a particle induced current to measure a combination of number concentration, lung deposited surface area (LDSA) concentration or the mean particle size. Two identical Nanoparticle Surface Area Monitors (NSAM, TSI model 3550, Fissan et al., 2007; Shin et al., 2007) were involved in the study. In an NSAM, particles are charged in an opposed flow unipolar diffusion charger (Medved et al., 2000; Kaminski et al., 2012), before ions are removed in an ion trap. The ion trap voltage can be triggered to manipulate the particle size distribution in a way that the current which is eventually measured in a Faraday cup electrometer (FCE) downstream of the ion trap is proportional to the fraction of the airborne particle surface area concentration that would deposit either in the alveolar or the tracheobronchial region of the human lung. Only the alveolar setting was used in this study.

Table 2
Overview of size-integrating concentration monitors and their settings in the study.

Manufacturer & model no.	Instrument ID	Metric	Size range (nm)	Concentration range	Time resolution (s)	Flow rate (lpm)	Accuracy [a]
TSI, 3776	CPC	NC[f]	>2.5	$<300{,}000$ #/cm^3 [b]	1	1.5	$\pm 10\%$
TSI, 3550	NSAM1, NSAM2	LDSA[g]	10–1000	$<10{,}000$ μm^2/cm^3 [c]	1	2.5	$\pm 20\%$ or 0.5 μm^2/cm^3 [c]
Fachhochschule Nordwestschweiz	miniDiSC1 to miniDiSC5	NC[f]	10–300 [d]	10^3–10^6 #/cm^3	1	1	$\pm 30\%$
		LDSA[g]	10–300 [d]				$\pm 30\%$
		MPS[h]	10–300 [d]				$\pm 30\%$
Philips Aerasense	nanoTracer1 to nanoTracer4	NC[f]	20–120 [d]	$<10^6$	16 /3 [e]	0.3–0.4	± 1500 #/cm^3
		MPS[h]	20–120 [d]				± 10 nm
Grimm, 1.320	nanoCheck	NC[f]	25–300 [d]	5×10^2 to 5×10^5 #/cm^3	10	1.2	$\pm 5\%$
		MPS[h]	25–300 [d]				$\pm 5\%$

[a] As specified by manufacturer.
[b] Single particle counting mode.
[c] For alveolar deposition.
[d] Modal diameters.
[e] With 3 s resolution only number concentration.
[f] NC=number concentration.
[g] LDSA=lung deposited surface area concentration.
[h] MPS=mean particle size.

The instrument uses a 1 μm cut-off cyclone at its inlet and is supposed to measure LDSA from this size down to 10 nm. Based on calibration with monodisperse particles it was shown that the calibration is only valid for particle sizes between 20 nm and 400 nm (Asbach et al., 2009b). The use of a pre-separator with lower cut-off size has hence been suggested (Asbach et al., 2011). Its use, however, was not possible here, because it requires modifications of the flow control.

Five identical miniature diffusion size classifiers (miniDiSC, University of Applied Sciences and Arts Northwestern Switzerland, Fierz et al., 2011; meanwhile commercially available as DiSCmini from Matter Aerosol, Wohlen, Switzerland) were used. In the miniDiSC, particles get charged in a unipolar diffusion charger, before they are passed on to a dual stage particle deposition system. The first stage contains a diffusion screen, where particles are deposited with a size-dependent efficiency. The second stage contains a high efficiency filter, on which all particles that penetrated the first stage are captured. Both stages are connected to FCEs that continuously measure the current, induced by the deposited particles. With these two independent measurements, the particle number concentration and the mean particle size are derived with 1 s time resolution. The instrument is designed to measure in a size range from 10 nm to 300 nm and a concentration range from 10^3 to 10^6 #/cm^3. In addition, the instrument exploits the fact that from approximately 20 nm to 400 nm, the LDSA and the charging efficiency of the miniDiSC charger follow nearly the same size dependence. Therefore the total current on both stages is proportional to the LDSA. The miniDiSC is equipped with an impactor with a cut-off at around 700 nm.

Altogether four nanoTracers (Philips Aerasense, Eindhoven, The Netherlands (Marra et al., 2010)) were included in the study. In a nanoTracer, particles also get unipolarly charged in a diffusion charger. The size distribution is then manipulated in a low-efficiency electrostatic precipitator (ESP) with an applied square-wave voltage. The particle induced current is eventually measured in an FCE. The number concentration and mean particle size are derived from the two different currents, measured during high and low voltage applied to the precipitator. One of the four nanoTracers (nanoTracer-3) used in this study was a simplified version that does not apply a square-wave voltage to the ESP, but instead only measures the total current from the particles and assumes a constant average particle diameter of 50 nm to calculate the number concentration from the measured current. The number concentration is then calculated from the measured current by using this constant particle size. This version of the nanoTracer is also referred to as nanoMonitor. The nanoTracers were set to deliver different time resolutions of 10, 13, 16 s and 20 s, respectively. According to the manufacturer's specifications, the instrument is designed for total concentrations below 10^6 #/cm^3 and modal diameters between 20 nm and 120 nm. Unlike the miniDiSC, the nanoTracer uses a small fan to establish the sample flow rate and therefore does not allow for the use of a pre-separator.

One nanoCheck (Grimm Aerosoltechnik, model 1.320) was employed in the study. The instrument uses the same principle as the nanoTracer, but with different data acquisition and evaluation software. The instrument operates at a total flow rate of 1.2 lpm and is designed to be used along with an optical spectrometer. It measures the number concentration and mean particle size in a size range from 25 nm to 300 nm and a concentration range from 500 to 5×10^5 #/cm^3 with 10 s time resolution. The nanoCheck uses a first stage to remove small particles below approximately 25 nm upstream of the charger, but no pre-separator to remove particles above 300 nm.

2.3. Data evaluation methods

2.3.1. Instruments measuring particle size distributions

As described above, different constant concentration levels were produced for each particle material for one hour per material and concentration. The size distributions measured by each of the instruments were then averaged for each of these one hour periods. The direct comparison of these averaged size distributions from the different instruments simply by plotting the distributions in a single graph is cumbersome and hinders direct comparisons. Different size bins and size resolutions of the instruments can lead to a distorted view on the distributions. If the measured concentrations are very different, the concentrations have to be plotted in different graphs, the same graph with several y-scales or normalized. All this only allows an optical comparison of the size distributions which is rather qualitative than quantitative. In the case of laboratory-generated aerosols as in the present study, a lognormal particle size distribution can be assumed (see Fig. 2). For a quantitative comparison of the measurement results, the measured size distributions were therefore fitted to lognormal distributions, using the least square fit method of Microsoft Excel 2003. The temporal variations of the size distributions were very small as indicated by the small error bars in Fig. 2 such that no further adjustment was necessary. The fitted size distributions could –if necessary – be extrapolated beyond the instruments' size ranges such that all distributions covered the same size range from 10 nm to 1000 nm. As a result the three parameters that determine a lognormal distribution, i.e., modal diameter d_{modal}, total number concentration C_N, and the geometric standard deviation σ_g can be derived comparably to each other, which is otherwise not necessarily the case. The coefficient of determination R^2 of each fit provided insight into the quality of the fitting procedure. The same approach has been used in the past for a similar study (Asbach et al., 2009a).

2.3.2. Instruments measuring size-integrated concentrations

The comparison of total concentrations by optically comparing concentration time series is more qualitative than quantitative, similar to the comparison of size distributions. Instead, a regression analysis in which the data from the one instrument is plotted against the data from a reference instrument provides a clearer picture. This is the same procedure

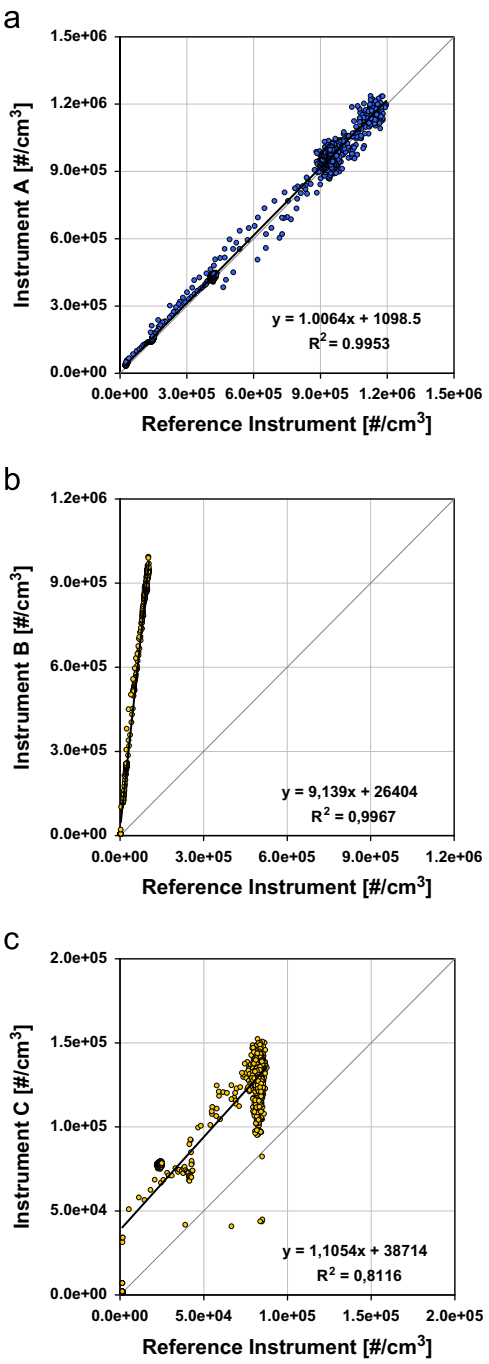

Fig. 3. Examples for regression analyses, (a) very good comparability, (b) very good correlation, but low agreement, (c) poor comparability.

that has been used in a different study on the comparison of portable nanoparticle exposure monitors (Asbach et al., 2012). Results from instruments that have identical time resolutions can be directly used for this comparison. If two instruments with different time resolution are to be compared, either the resolution of the instrument with higher time resolution needs to be reduced or the resolution of the other instrument artificially increased. An artificial increase of the time resolution can be achieved by linear interpolation between the data points. This was done here to increase the time resolution of the nanoCheck and nanoTracer to a virtual resolution of 1 s.

Regression analyses were carried out by linear fit for each size-integrating instrument and particle material separately. The fit data, i.e., slope and *y*-intersect are used to describe the comparability of the measurement. Ideal comparability means that all data points fall onto the 1:1 line, i.e., the slope of the fit is one and the *y*-intersect zero, while the coefficient

of determination is one. Three examples for this methodology are shown in Fig. 3. The top graph Fig. 3a shows an example for good comparability of the number concentration from an instrument A compared with the reference instrument. The slope of the linear fit is 1.0064, hence the devices agreed on average to within 0.64%. The y-intersect of $+1098.5$ amounts to only approximately 1% of the total concentration range and can hence be considered as rather low. The coefficient of determination is 0.9953 and hence very close to one, indicating the high linear correlation of the two instrument readings. Fig. 3b shows an example of highly correlated but poor agreement. The correlation between instrument B and the reference instrument is 0.9967 (R^2), but the slope 9.139. This indicates that the concentration readings of instrument B are about a factor 9 higher than those of the reference instrument. The y-intersect amounts to approximately 2.5% of the total concentration range, which can be considered acceptable. Fig. 3c shows another example for poor comparability of an instrument C with the reference instrument, in this case for soot particles. Although the slope is rather close to one, the y-intersect amounts to approximately 35% of the total concentration range showing a significant offset. The relatively low R^2 of 0.8116 reflects the unstable reading of instrument C (95,000–150,000 #/cm^3) during relatively stable particle number concentration around 80,000 #/cm^3. Average concentrations and standard deviations were calculated for each instrument during episodes with constant concentrations in the mixing chamber for comparison additionally to the regression analysis.

The geometric mean diameters were calculated from measurements with the internal reference SMPS (SMPS-G1) for comparison with mean particle sizes reported by miniDiSC, nanoTracer and nanoCheck. The mean particle sizes from these instruments were averaged over the times of constant concentrations for each test aerosol.

In the case of the measurement of LDSA concentrations, the results from instruments measuring this quantity directly were plotted against data from NSAM-1 and parameters of the regression analyses determined. Since the NSAM uses an indirect measurement principle to determine the LDSA concentration, the average LDSA concentrations during each one hour run were additionally compared with those calculated from size distributions measured with SMPS. To do so, initially the surface area size distribution is calculated from the number size distribution and then multiplied with the corresponding lung deposition curve, here for deposition in the alveolar region. The particle size dependent deposition rates can be obtained from a model, published by the International Commission on Radiological Protection (ICRP, publication 66, 1994). While this procedure is straightforward for spherical particles, the relationship between electrical mobility diameter and both the surface area and the lung deposition rates of agglomerated particles are usually unknown. However, Fissan et al. (2012) calculated the surface area size distribution of agglomerated particles based on a model by Lall & Friedlander (2006) and based on the assumption of spherical particles by using the mobility diameter as the geometric diameter and a particle density of 1000 kg/m^3. The observed differences depend on the particle size, but were always found to be at most on the order of a few percent and hence concluded to be negligibly small. In the particle size range below approximately 300 nm, lung deposition of particles is mainly driven by Brownian motion, which can best be described by the mobility diameter. We therefore calculated LDSA concentrations here by using the electrical mobility diameter as the "true" particle diameter and a particle density of 1000 kg/m^3. Fissan et al. (2012) showed in their study that a good comparability between NSAM and SMPS data can be achieved this way.

3. Results and discussion

3.1. Instruments measuring size distributions

The normalized particle number size distributions of the test aerosols are shown in Fig. 2. The measured size distributions from all instruments were fitted to lognormal distributions and analyzed as described above.

3.1.1. Comparison of SMPSs

The parameters of the fitted lognormal SMPS size distributions for all experimental runs are given in Table 3. In the first experimental run with NaCl particles, two different particle concentrations were sequentially measured for one hour each, namely on average 14,700 #/cm^3 with NaCl-1 and 94,600 #/cm^3 with NaCl-2 (data from CPC). All fitted size distributions are shown in Fig. 4. Total number concentrations of the fitted SMPS-G1 curves were 14,600 #/cm^3 and 91,000 #/cm^3, respectively, hence deviating only 0.5% and 3.8% from the CPC concentration. Modal diameters, from SMPS-G1 were 42.2 nm (NaCl-1) and 37.0 nm (NaCl-2) with GSDs of 1.72 and 1.66, respectively. The modal diameters reported by the Grimm and TSI SMPSs for sodium chloride particles are all within a very narrow range between 38.1 nm and 42.2 nm for NaCl-1 and between 33.6 nm and 37.0 nm for NaCl-2. This shows the very good sizing agreement of the SMPSs to within $\pm 5\%$ for the sodium chloride test aerosols. The geometric standard deviations showed variations between 1.72 and 1.94 (NaCl-1) and between 1.66 and 1.77 (NaCl-2), i.e., in a similarly narrow range. These findings are in good agreement with a previous study by Asbach et al. (2009a), who compared the results of TSI SMPSs, Grimm SMPSs and an FMPS when challenged with laboratory generated NaCl and diesel soot particles, using the same facility as in the present study. They found a good general sizing agreement between Grimm SMPSs equipped with long and short DMA as well as between TSI SMPSs with identical settings.

The reported number concentrations, however, showed a larger variability between instruments. Total number concentrations from SMPSs were compared with those from the CPC. Although the CPC covers a wider size range than the SMPSs, all particle size distributions were such that they are well within the SMPS size ranges and hence contributions

Table 3
Parameters of the fitted SMPS size distributions and their deviations from SMPS-G1 (modal diameter and geometric standard deviation) and from CPC (number concentration).

Instrument ID		NaCl				DEHS				Soot					
		1		2		1		2		1		2		3	
			Deviation [a]		Deviation [a]		Deviation [a]		Deviation [a]		Deviation [a]		Deviation [a]		Deviation [a]
SMPS-G1	d_{modal} [nm]	**42.2**	–	**37.0**	–	**263.3**	–	**239.8**	–	**105.9**	–	**99.8**	–	**58.8**	–
	GSD	**1.72**	–	**1.66**	–	**1.93**	–	**1.71**	–	**1.54**	–	**1.53**	–	**1.56**	–
	C_N [#/cm^3]	**14,627**	−0.5%	**90,964**	−3.8%	**21,614**	−5.4%	**101,186**	0.7%	**26,419**	12.5%	**89,148**	7.3%	**91,894**	12.5%
SMPS-G2	d_{modal} [nm]	**39.6**	−6.2%			**243.5**	−7.5%	**229.6**	−4.2%	**104.5**	−1.4%	**97.5**	−2.2%	**57.0**	−3.1%
	GSD	**1.79**	4.1%			**1.97**	2.1%	**1.7**	−0.6%	**1.55**	0.6%	**1.55**	1.3%	**1.58**	1.3%
	C_N [#/cm^3]	**15,588**	6.1%			**18,536**	−18.8%	**86,292**	−14.2%	**25,452**	8.4%	**89,437**	7.6%	**91,488**	12.0%
SMPS-G3	d_{modal} [nm]	**38.1**	−9.7%	**36.5**	−1.3%	**256.9**	−2.4%	**234.9**	−2.0%	**109.9**	3.7%	**103.3**	3.6%	**61.1**	3.9%
	GSD	**1.81**	5.2%	**1.73**	4.2%	**1.88**	−2.6%	**1.66**	−2.9%	**1.53**	−0.6%	**1.52**	−0.7%	**1.56**	0.0%
	C_N [#/cm^3]	**20,588**	40.1%	**116,610**	23.3%	**31,851**	39.5%	**139,066**	38.3%	**35,151**	49.7%	**118,674**	42.8%	**114,830**	40.6%
SMPS-G4	d_{modal} [nm]	**42.9**	1.7%	**36.3**	−1.7%	**264.9**	0.6%	**235.8**	−1.7%	**110.2**	4.0%	**92.9**	−6.9%	**55.1**	−6.4%
	GSD	**1.94**	12.8%	**1.73**	4.2%	**1.81**	−6.2%	**1.64**	−4.1%	**1.53**	−0.6%	**1.51**	−1.3%	**1.56**	0.0%
	C_N [#/cm^3]	**10,640**	−27.6%	**120,280**	27.2%	**33,313**	45.9%	**153,589**	52.8%	**36,973**	57.5%	**128,940**	55.2%	**125,033**	53.1%
SMPS-G5	d_{modal} [nm]	**40.7**	−3.7%	**35.5**	−4.1%	**159.0**	−39.6%	**164.5**	−31.4%	**106.2**	0.2%	**100.3**	0.5%	**59.0**	0.3%
	GSD	**1.76**	2.3%	**1.68**	1.2%	**1.82**	−5.7%	**1.55**	−9.4%	**1.52**	−1.3%	**1.51**	−1.3%	**1.56**	0.0%
	C_N [#/cm^3]	**15,219**	3.6%	**94,497**	−0.1%	**11,176**	−51.1%	**51,775**	−48.5%	**30,188**	28.6%	**102,879**	23.8%	**101,789**	24.6%
SMPS-T1	d_{modal} [nm]	**40.3**	−4.5%	**34.8**	−5.8%	**302.0** [b]	14.7%	**258.5** [b]	7.8%	**102.7**	−3.1%	**97.4**	−2.4%	**57.8**	−1.8%
	GSD	**1.78**	3.5%	**1.71**	3.0%	**2.05** [b]	6.2%	**1.75** [b]	2.3%	**1.53**	−0.6%	**1.52**	−0.7%	**1.56**	0.0%
	C_N [#/cm^3]	**14,156**	−3.7%	**95,258**	0.7%	**20,996** [b]	−8.1%	**95,262** [b]	−5.2%	**28,003**	19.3%	**97,959**	17.9%	**93,460**	14.4%
SMPS-T2	d_{modal} [nm]	**39.5**	−6.5%	**33.6**	−9.0%	**296.0**	12.4%	**251.8**	5.0%	**108.8**	2.7%	**101.7**	1.9%	**58.7**	−0.2%
	GSD	**1.8**	4.7%	**1.77**	6.6%	**2.08**	7.8%	**1.73**	1.2%	**1.54**	0.0%	**1.53**	0.0%	**1.58**	1.3%
	C_N [#/cm^3]	**13,651**	−7.1%	**96,896**	2.4%	**18,778**	−17.8%	**81,635**	−18.8%	**20,498**	−12.7%	**77,789**	−6.4%	**80,731**	−1.2%
SMPS-T3	d_{modal} [nm]	**39.9**	−5.4%	**36.4**	−1.6%	**292.3**	11.0%	**248.7**	3.7%	**108.8**	2.7%	**101.9**	2.1%	**60.3**	2.6%
	GSD	**1.8**	4.7%	**1.71**	3.0%	**2.01**	4.1%	**1.73**	1.2%	**1.53**	−0.6%	**1.53**	0.0%	**1.55**	−0.6%
	C_N [#/cm^3]	**14,052**	−4.4%	**85,193**	−9.9%	**19,964**	−12.6%	**86,388**	−14.1%	**20,458**	−12.9%	**69,746**	−16.1%	**70,498**	−13.7%
CPC	C_N [#/cm^3]	**14,696**	–	**94,582**	–	**22,839**	–	**100,520**	–	**23,481**	–	**83,091**	–	**81,681**	–

C_N: deviation from reference CPC.
[a] d_{modal} and *GSD*: deviation from reference SMPS-G1.
[b] Manual multiple charge correction.

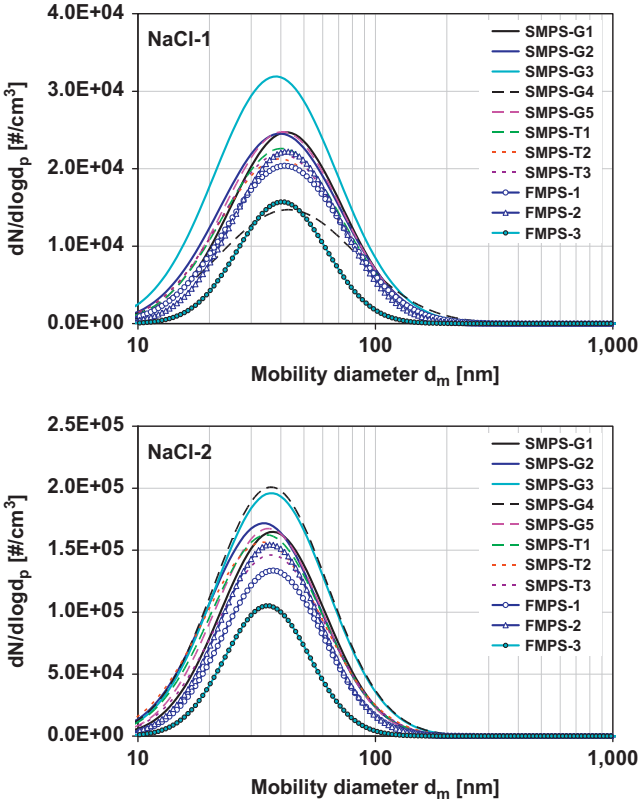

Fig. 4. Fitted NaCl size distributions from SMPSs and FMPSs.

from particles in the non-overlapping size range to the total number concentrations were negligibly small. All TSI SMPSs showed concentrations between 9.9% below and 0.7% above the CPC concentration, independent of the SMPS flow rates. On the contrary, Asbach et al. (2009a) reported that increasing the flow rates in one TSI SMPS resulted in higher concentrations. Out of the Grimm SMPSs, SMPS-G1, SMPS-G2 and SMPS-G5 agreed similarly well with the CPC concentrations as the TSI instruments. The concentrations reported by SMPS-G3 and SMPS-G4 were between 23.3% and 40.1% higher than the CPC concentration, except for SMPS-G4 which during NaCl-1 measurement showed 27.6% lower concentration. It should be noted that these two SMPS were operated with an older software version. Asbach et al. (2009a) showed the same trend between a Grimm SMPS with the old software version and TSI SMPSs. Similar results were also reported by Helsper et al. (2008). The reason for the underestimation of the number concentration by SMPS-G4 during NaCl-1 measurement remains unclear. It may be possible that inaccurate flow rates may have caused this discrepancy. The need for very careful control over flow rates has also been reported elsewhere (Dahmann, 1997; Asbach et al., 2009a).

Two different DEHS concentrations with very similar modal diameters were produced. DEHS-1 had a modal diameter of 263 nm (from SMPS-G1) and a total number concentration of 22,800 #/cm^3 (from CPC) and DEHS-2 a modal diameter of 240 nm and 100,500 #/cm^3, respectively. The size distributions are shown in Fig. 5. During the DEHS measurements the size distributions measured with Grimm SMPS with short DMA (SMPS-G5) consistently dropped well below the size distributions from all other instruments for particle sizes above approximately 150 nm, despite the fact that the instrument should measure accurately up to 350 nm. A similar trend was also observed by Watson et al. (2011), who compared the results from two TSI SMPSs, one with a long DMA the other with a nano-DMA, a Grimm SMPS+C with short DMA and an MSP SMPS during a one month measurement campaign at the Fresno Supersite in California. The geometric mean diameter measured with the TSI SMPS with long DMA was consistently larger than that measured by Grimm SMPS with short DMA. They concluded that deviations in the results from SMPS instruments may stem from differences in particle charging efficiency, CPC counting efficiency, diffusion losses, and non-ideal DMA transfer functions. As a result of the discrepancy between the DEHS size distributions measured with SMPS-G5 with short DMA and all other SMPSs, SMPS-G5 data were therefore not further evaluated for DEHS aerosol. For all other SMPSs the comparability for sizing as well as for the total concentration was lower compared to the NaCl aerosol. The agreement was best with SMPS-G1 with −5.4% and +0.7% deviation from the CPC concentration for DEHS-1 and DEHS-2, respectively. SMPS-G2, which was largely identical with SMPS-G1 delivered 18.8% (DEHS-1) and 14.2% lower concentrations than the CPC whereas SMPS-G3 and SMPS-G4 measured between 38.3% and 52.8% higher concentrations. The latter finding is in agreement with the NaCl measurements as well as with previously published results (Asbach et al., 2009a) and hence strengthen the suspicion that

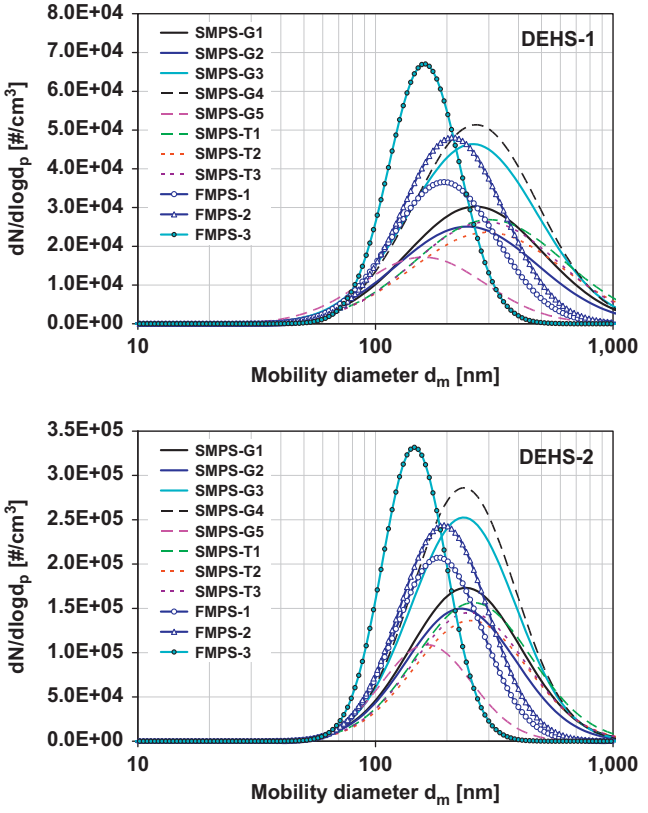

Fig. 5. Fitted DEHS size distributions from SMPSs and FMPSs.

the older software version (see Table 1) over-estimates the total particle number concentration. Out of the TSI SMPSs, the one operated with higher flow rates (SMPS-T1) showed the best agreement with 7.8% and 5.0%, respectively, lower concentrations than the CPC. SMPS-T1 and SMPS-T2 measured between 12.6% and 18.8% lower concentrations than the CPC. It should be noted that SMPS-T1 was operated with a pre-impactor with a significantly too large cut-off diameter (nozzle size 0.071 cm, $d_{p,50}=1027$ nm for DEHS density 914 kg/m^3). The multiple charge correction of the AIM software was therefore not meaningfully useable. Instead, in order to obtain the results given for SMPS-T1 in Table 3, the measured mobility distribution was artificially extrapolated, following a lognormal distribution and the multiple charge correction carried out manually by using the principle introduced by Hoppel (1978) along with the Wiedensohler (1988) charge approximation. The comparability of the sizing was also worse for the DEHS aerosol compared with NaCl aerosol. Although the Grimm SMPSs agreed to within $\pm 4.2\%$ (DEHS-1) and $\pm 2.2\%$ (DEHS-1) with each other and the TSI SMPS to within $\pm 1.6\%$ and $\pm 1.9\%$, respectively, the modal diameters reported by the TSI SMPSs was between 11.1% and 14.7% (DEHS-1) and between 3.7% and 7.8% (DEHS-2) larger than those reported by SMPS-G1. It is interesting to note that for the larger DEHS particles TSI SMPSs report larger sizes, whereas for the smaller NaCl particles it was vice versa. Multiple charge correction (MCC) is a possible explanation for the observed discrepancies, because it affects both the sizing and the concentration determined with an SMPS. Small particles, as in the case of the NaCl aerosol, leaving the DMA are almost completely singly charged and MCC hence does not affect the measured distribution. In the case of the larger DEHS particles, the fraction of multiply charged particles in the mono-mobile fraction exiting the DMA is significantly higher and needs to be corrected using the MCC. The SMPSs from the two manufacturers use different neutralizers, ^{85}Kr in the case of TSI and ^{241}Am in the case of Grimm and different polarities in the DMA, i.e., TSI uses a negative voltage to select positively charged particles, whereas Grimm uses positive voltage to select negatively charged particles. Both instruments use the same set of equations to predict the charge distributions (Wiedensohler, 1988), but with different coefficients to account for the different polarities. Small differences in the effective charge distributions from the different neutralizers can therefore result in differences in the multiple charge corrected size distributions. The reported geometric standard deviations were consistently slightly smaller with Grimm SMPSs compared with TSI SMPSs.

Three different soot aerosols were produced with the spark generator (Palas GFG-3000). The total generator current was always 14.6 mA and the argon flow rate approximately 8.5 lpm. The generator allows for a dilution of the freshly produced aerosol with particle-free dilution air to avoid rapid coagulation. In the case of soot-1, the aerosol remained undiluted, in the case of soot-2, 2 lpm dilution air were added and 15 lpm in the case of soot-3. The highly concentrated aerosol was further diluted in the wind tunnel with 1044 m^3/h filtered air in the case of soot-1 and with 325 m^3/h in the

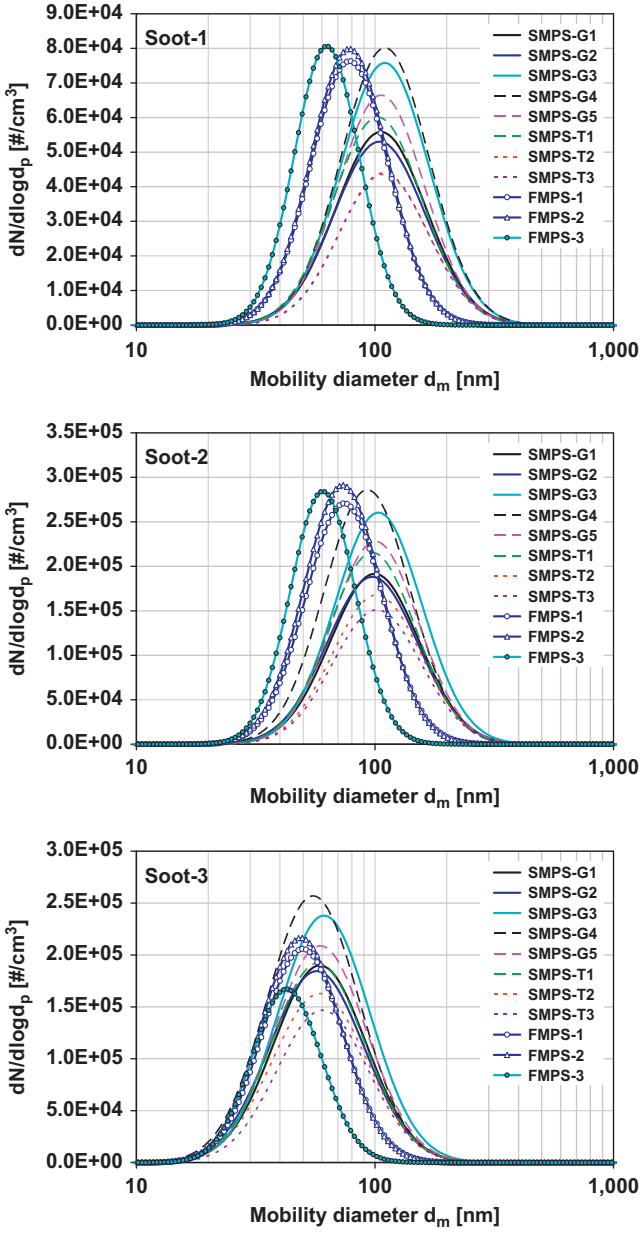

Fig. 6. Fitted soot size distributions from SMPSs and FMPSs.

case of soot-2 and soot-3. The resulting size distributions in the measurement chamber had modal diameters of 106 nm, 100 nm and 59 nm (from SMPS-G1) for soot-1, soot-2 and soot-3, respectively with total number concentrations of 23,500 #/cm^3, 83,100 #/cm^3 and 81,700 #/cm^3 (from CPC). All soot size distributions are shown in Fig. 6. The agreement of the sizing was again excellent, with reported modal diameters from all instruments in a range of $\pm 4\%$ for soot-1, $\pm 3\%$ for soot-2 and $\pm 4\%$ for soot-3 (only SMPS-G4 sometimes showed slightly higher deviations). The measured geometric standard deviations reported by the different SMPSs were almost identical. The variation of the measured number concentrations was significantly higher, ranging from -1.2% (SMPS-T2 with soot-3) to $+57.9\%$ (SMPS-G4 with soot-2). No clear trend can be seen depending on the particle size or concentration, but again the older Grimm software produced the highest deviations. While the instruments with the newer software reported only between 8.4% and 12.5% higher concentrations than the CPC, the older software over-estimated the concentration between 24.6% and 57.9%. The TSI SMPS with 0.6/6 lpm aerosol to sheath flow (SMPS-T1) read higher concentrations than the SMPSs with 0.3/3 lpm. SMPS-T1 concentrations were between 14.4% and 19.3% higher than the CPC, whereas SMPS-T2 and SMPS-T3 concentrations were between 1.2% and 16.1% below the CPC readings. The fact that the sizing agrees very well whereas the concentration

Table 4
Parameters of the fitted FMPS size distributions and their deviations from SMPS-G1 (modal diameter and geometric standard deviation) and from CPC (number concentration).

Instrument ID		NaCl				DEHS				Soot					
		1		2		1		2		1		2		3	
			Deviation [a]		Deviation [a]		Deviation [a]		Deviation [a]		Deviation [a]		Deviation [a]		Deviation [a]
FMPS-1	d_{modal} [nm]	**41.6**	−1.5%	**37.0**	0.1%	**194.2**	−26.2%	**184.9**	−22.9%	**78.3**	−26.1%	**74.4**	−25.5%	**49.8**	−15.3%
	GSD	**1.77**	2.9%	**1.62**	−2.4%	**1.66**	−14.0%	**1.52**	−11.1%	**1.45**	−5.8%	**1.46**	−4.6%	**1.47**	−5.8%
	C_N [#/cm^3]	**12,623**	−14.1%	**70,529**	−25.4%	**20,196**	−11.6%	**94,821**	−5.7%	**31,159**	32.7%	**110,597**	33.1%	**86,831**	6.3%
FMPS-2	d_{modal} [nm]	**42.3**	0.1%	**36.2**	−2.1%	**211.3**	−19.7%	**193.4**	−19.3%	**78.1**	−26.3%	**73.2**	−26.6%	**49.0**	−16.8%
	GSD	**1.67**	−2.9%	**1.61**	−3.0%	**1.64**	−15.0%	**1.54**	−9.9%	**1.45**	−5.8%	**1.45**	−5.2%	**1.47**	−5.8%
	C_N [#/cm^3]	**12,447**	−15.3%	**80,431**	−15.0%	**25,886**	13.3%	**114,497**	13.9%	**32,438**	38.1%	**118,545**	42.7%	**91,482**	12.0%
FMPS-3	d_{modal} [nm]	**40.5**	−4.1%	**35.1**	−4.9%	**160.7**	−39.0%	**145.8**	−39.2%	**62.8**	−40.7%	**60.5**	−39.4%	**42.6**	−27.5%
	GSD	**1.54**	−10.5%	**1.51**	−9.0%	**1.41**	−26.9%	**1.37**	−19.9%	**1.37**	−11.0%	**1.37**	−10.5%	**1.40**	−10.3%
	C_N [#/cm^3]	**7,380**	−49.8%	**47,034**	−50.3%	**25,208**	10.4%	**112,440**	11.9%	**27,726**	18.1%	**97,452**	17.3%	**61,212**	−25.1%

C_N: deviation from reference CPC.
[a] d_{modal} and *GSD*: deviation from reference SMPS-G1.

measurement does not, may again be explained by the charging of the different neutralizers. The fraction of multiply charged particles in the 60 nm and 100 nm mobility size bin according to Fuchs theory (Fuchs, 1963) and its approximation by Wiedensohler (1988) is still very small (only $\approx 2.5\%$ of 88 nm and $\approx 5.5\%$ of 151 nm particles are doubly charged and have the same electrical mobility as singly charged 60 nm and 100 nm particles, respectively). Therefore the MCC does not very much shift the distributions on the diameter axis, but on the concentration axis due to the eventual division by the probability of singly charged particles. Differences in the charging efficiency of spheres (assumed in the model) and agglomerates (as for soot) hence mainly result in errors in the determination of the concentration, but not so much in the size.

3.1.2. Comparison of FMPSs

Three Fast Mobility Particle Sizers were tested alongside the SMPSs. In general, the FMPS is a very fast reading electrical mobility spectrometer with 1 s time resolution. However, the downside is a reduction in size resolution and lower accuracy. All measured particle size distributions were fitted to lognormal size distributions and evaluated as described above. The lognormal fit data of the FMPS size distributions are given in Table 4 along with deviations from SMPS-G1 and CPC, respectively. It can be seen from the table as well as the size distributions shown in Fig. 4 that the sizing agreement among FMPSs for sodium chloride particles was always very good with deviations of the modal diameter on the order of only $\pm 2\%$. In addition the modal diameters agree very well with those reported by SMPS-G1. The geometric standard deviations were also in acceptable agreement with those reported by SMPS-G1 with only FMPS-3 delivering a noticeably narrower distribution. Similarly good agreement between FMPS and a TSI SMPS for ammonium sulphate particles of similar sizes (geometric mean diameter of 32 nm) was also reported by Leskinen et al. (2012). All FMPSs measured lower total number concentrations than the CPC. While the deviations of FMPS-1 and FMPS-2 from the CPC were between -14.1% and -25.4%, the FMPS-3 concentrations were about a factor of two lower than the CPC concentration during NaCl-1 and NaCl-2 measurements.

The size distributions (shown in Fig. 5) measured with the FMPSs for the DEHS aerosols were significantly shifted towards smaller particles sizes compared to the SMPS-G1 size distributions. In addition all FMPS distributions were noticeably narrower. The deviations were particularly pronounced for FMPS-3, which gave modal diameter readings lower by 39% for both DEHS concentrations. Geometric standard deviations for FMPS-3 were smaller by 26% (DEHS-1) and 20% (DEHS-2). The deviations from SMPS-G1 were lower but still significant and followed the same trend with FMPS-1 and FMPS-2. During DEHS-1 measurement, FMPS-1 and FMPS-2 under-estimated the modal diameter by 26% and 20%, respectively, and the width by 14% and 15%. During DEHS-2 measurements, the modal diameter was under-represented by 23% and 19% and the GSD by 11% and 10%, respectively. Interestingly, the agreement between the total number concentrations from all FMPSs and the CPC was better and on the order of $\pm 14\%$. The finding with DEHS and NaCl aerosols show that the FMPS agreement with SMPSs concerning sizing as well as the concentration measurement obviously strongly depends on particle size. While the sizing agreement between SMPS-G1 and FMPS was excellent for sodium chloride particles with sizes around 40 nm, it was rather poor with DEHS particles with sizes round 250 nm. This discrepancy may be caused by the fact that particles in a unipolar diffusion charger, as used in the FMPS, acquire a charge level which is nearly proportional to the particle diameter (Asbach et al., 2011; Jung & Kittelson, 2005). The Cunningham slip correction factor (Cunningham, 1910; Kim et al., 2005; Jung et al., 2012) is becoming an increasingly weak function of particle diameter with increasing particle size and hence the electrical mobility of unipolarly diffusion charged particles also is getting less and less sensitive to the particle diameter. As a result, unambiguous differentiation of differently sized particles based on electrical mobility analysis is becoming more and more difficult.

The FMPSs showed the worst agreement for agglomerated soot particles (size distributions shown in Fig. 6). Again FMPS-3 showed the highest deviations, under-representing the modal diameters by approximately 40% in the case of soot-1 and soot-2 and by 28% in the case of soot-3 compared with SMPS-G1. For soot-1 and soot-2, FMPS-3 reported approximately 19% higher concentrations than the CPC, whereas for soot-3 it was about 25% lower. Geometric standard deviations from FMPS measurements were on average 11% smaller than those from SMPS-G1. Since FMPS-3 showed the highest deviations during all experimental runs with all three materials it is assumed that the device itself was faulty and hence not representative. However, also FMPS-1 and FMPS-2 size distributions were noticeably shifted towards smaller particle sizes. Modal diameters during soot-1 and soot-2 measurements were in all cases approximately 26% and during soot-3 measurement approximately 16% smaller than those measured with SMPS-G1. Geometric standard deviations were on average 5% lower. Total number concentrations from FMPS-1 and FMPS-2 were 33% and 38% higher than the CPC concentration for soot-1 and 35% and 45% for soot-2. For soot-3 the agreement was better with only 6.3% and 12%, respectively, higher concentrations. In all above cases the agreement was worse for the larger soot particles (soot-1 and soot-2, modal diameter around 100 nm) than for the smaller one (soot-3, 60 nm). These findings are in very good agreement with results by Leskinen et al. (2012), who studied the response of FMPS and SMPS to agglomerated TiO_2 particles of different sizes and from different sources. They also reported that the FMPS produced smaller particle sizes with narrower distributions and higher concentrations than a TSI SMPS and that the effect was more pronounced when the agglomerates were larger. The inaccuracy of the FMPS when measuring agglomerated particles hence seems to be a systematic problem of the FMPS and not just of the specific specimens used here. The agreement for the 60 nm soot particles was much worse than for 40 nm NaCl particles. This indicates that the FMPS accuracy not only shows dependence on the particle size as pointed out with the DEHS measurements but also on particle morphology, because as the soot

particles got smaller, the inaccuracy caused by the particle size decreased, whereas the inaccuracy caused by particle morphology remained. A likely reason for inaccuracies caused by particle morphology is the different charge level, particles acquire in the unipolar charger of the FMPS dependent on their morphology. This was also hypothesized by Asbach et al. (2009a) in their earlier study with diesel soot particles. They also showed that an FMPS reported smaller count median diameters and narrower distributions than all SMPSs in their test although it seems that the effect was less pronounced than here. The reason for the less pronounced effect may be that freshly emitted diesel soot particles are often covered with volatile organic compounds, likely giving the particles a more compact shape while airborne than the spark-generated pure-carbon soot particles used in the present study.

The discrepancies between FMPS and SMPS readings found here are in general agreement with those reported by Asbach et al. (2009a). In their case, the size distributions delivered by the FMPS were consistently shifted to smaller particles for both tested particle materials. For sodium chloride particles, the FMPS number concentration was almost identical with the TSI SMPS number concentration, but for soot particles, it was between 30% and 70% higher. It was suspected that different charging probabilities of the bipolar (SMPS) and unipolar (FMPS) charger caused the differences for the differently shaped particles of NaCl and diesel soot. Jeong and Evans (2009) also found similar deviations between a TSI SMPS and FMPS and suggested the use of a size dependent correction factor for better comparison of SMPS and FMPS size distributions. Both studies described the recurrent presence of obviously artificial peaks in the FMPS size distributions around 10 nm that were also seen in the present study in all FMPSs. These peaks seem to appear randomly and at various heights, that are usually well below the main peak of the measured size distribution. The reasons for these peaks even after discussions with the manufacturer, remain unclear, but seem to represent a systematic instrument failure.

3.2. Instruments measuring size-integrated concentrations

All diffusion charger based instruments measuring size-integrated particle number concentrations measured the same aerosol alongside the electrical mobility spectrometers and the CPC. Two types of analyses were conducted with the results. First, the number or lung deposited surface area concentrations were plotted against the simultaneously measured number concentrations measured with the CPC or LDSA concentrations measured with NSAM-1, respectively, similar to the examples shown in Fig. 3, and fitted. Second, the reported number or LDSA concentrations, as well as the mean particle sizes were averaged and standard deviations calculated for each particle material over the 1 h periods of constant concentration.

miniDiSC, nanoTracer and nanoCheck as well as Aerotrak9000 (TSI, largely identical with NSAM) have been subject to a recent study on their comparability, when challenged with sodium chloride, DEHS and soot particles (Asbach et al., 2012). This study showed that in general, diffusion charger based instruments have many practical advantages, but a lower accuracy than e.g., CPCs. They reported that the comparability of diffusion charger based devices is usually on the order of $\pm 30\%$. Some exceptions were, however, noted. The nanoTracer reported up to a factor of about 7 higher number concentrations when challenged with DEHS aerosol with a modal diameter of nearly 200 nm, i.e., beyond the specified range for the instrument. This strong overestimation of the number concentration was likely caused by a misinterpretation of the measured current by the software. To the contrary, the nanoCheck underestimated the number concentration of soot particles by about 59%. These soot particles had a modal diameter of approximately 30 nm and it is thus likely that a large fraction of the particles was removed in the first particle removal stage of the nanoCheck. For all other materials, the concentrations as well as the mean particle sizes agreed within a margin of $\pm 30\%$.

3.2.1. Comparison of instruments measuring number concentration

Table 5 shows that for the number concentration, all devices delivered satisfactory agreement with the CPC for NaCl aerosol within the expected range of $\pm 30\%$, i.e., comparable to the recently reported results (Asbach et al., 2012). The miniDiSC regression analyses showed slopes between 0.88 and 1.01, showing that the largest error to be expected with this type of aerosols is on the order $\pm 12\%$. The largest y-intersect, i.e., offset, observed with miniDiSC-5 was around 2200 #/cm^3. Considering that the total concentration range in this regression analysis reached up to 95,000 #/cm^3, this amounts to approximately 2.5%. As Table 6 shows, the average number concentrations measured with the miniDiSCs and the CPC agreed to within $\pm 5\%$ for NaCl-1. With the higher concentration during NaCl-2 measurements, the deviation was slightly higher, but still below 12%. The measured miniDiSC and CPC data were all highly correlated with coefficient of determination of $R^2 > 0.99$. This finding agrees well with previously reported results (Asbach et al., 2012) which reported similarly good agreement between miniDiSC and handheld CPCs when challenged with NaCl aerosol, whereas Bau et al. (2012) reported agreement between the similar instrument meDiSC (Matter Aerosol, Switzerland) and a water based UCPC only on the order of $\pm 40\%$.

The agreement of the nanoTracers with the CPC was slightly lower. For the lower concentration (NaCl-1) the nanoTracers showed between 13% and 29% higher concentrations than the CPC. Only the concentrations measured by nanoTracer-3, i.e., the one that does not measure the mean particles size, but instead assumes it to be 50 nm, were increased by even approximately 57%. This is an interesting result, because the actual particle mean diameter was around 41 nm (see Table 6), i.e., close to the diameter assumed by the instrument. Still the correlation between CPC and nanoTracer-3 was very high with $R^2 = 0.989$. Considering the regression equation given in Table 5 for nanoTracer-3 with NaCl-1 it is obvious that the large offset of 6333 #/cm^3 caused this large error during measurements of low concentrations.

Table 5
Regression analyses; in the equations, y denotes the number concentration of the instrument named in the left column and x denotes the CPC number concentration; all concentrations in [#/cm^3].

Instrument ID	NaCl 1+2	DEHS 1+2	Soot 1+2	Soot 3
miniDiSC-1	$y=1.0064x+1098.5$ $R^2=0.9953$	$y=1.0369x+3,264.6$ $R^2=0.9904$	$y=1.2534x-855.5$ [a] $R^2=0.9836$	Failure
miniDiSC-2	$y=0.9292x+1426.1$ $R^2=0.9934$	$y=0.7646x-1,299.4$ $R^2=0.9952$	$y=1.0218x+1,383.9$ $R^2=0.9941$	$y=1.1179x-1,939.5$ $R^2=0.9904$
miniDiSC-3	$y=0.9660x+1374.1$ $R^2=0.9944$	$y=0.5479x-994.4$ $R^2=0.9941$	$y=0.9090x+501.9$ $R^2=0.9903$	$y=1.1064x-1,782.0$ $R^2=0.9516$
miniDiSC-4	$y=0.9926x+494.8$ $R^2=0.9947$	$y=0.6320x-1,536.7$ $R^2=0.9930$	$y=0.9881x+244.2$ $R^2=0.9923$	$y=1.1954x-5,404.9$ $R^2=0.9867$
miniDiSC-5	$y=0.8834x+2169.6$ $R^2=0.9925$	$y=0.4800x+911.0$ $R^2=0.9986$	$y=0.8638x+1,206.8$ $R^2=0.9921$	$y=1.0727x-2,917.1$ $R^2=0.9897$
nanoTracer-1	$y=1.0072x-2015.9$ $R^2=0.9951$	$y=9.1390x+26,403.7$ $R^2=0.9967$	$y=1.1054x+38,714.3$ $R^2=0.8116$	$y=0.9825x+16,645.7$ $R^2=0.8275$
nanoTracer-2	$y=0.7823x+4780.9$ $R^2=0.9909$	$y=2.4112x+12,647.9$ $R^2=0.9825$	$y=1.5747x+5,666.7$ $R^2=0.9859$	$y=1.4718x-327.4$ $R^2=0.9552$
nanoTracer-3	$y=0.9854x+6332.6$ $R^2=0.9890$	$y=14.2006x+70,682.0$ $R^2=0.9859$	$y=3.9268x+9,023.2$ $R^2=0.9833$	$y=1.9763x+4,677.5$ $R^2=0.6107$
nanoTracer-4	$y=1.1559x+2524.3$ $R^2=0.9954$	Failure	$y=1.7478x+1,342.1$ $R^2=0.9857$	$y=1.5176x-818.1$ $R^2=0.9620$
nanoCheck	$y=0.9032x+3121.6$ $R^2=0.9836$	$y=1.4269+2,137.4$ $R^2=0.7609$	$y=1.5953x+5,998.5$ $R^2=0.9877$	$y=0.7562x+65,463.1$ $R^2=0.0386$

[a] Soot-1 only.

Such an offset may have been caused by an improper electrometer zeroing, although no error messages were obtained from the instrument. This offset affects the measurement of low concentrations more strongly than high concentrations, as can be seen from the much better agreement between nanoTracer-3 and CPC for NaCl-2 at a concentration of around 95,000 #/cm^3. Here nanoTracer-3 showed on average only 5% higher concentrations. The agreement of the other three nanoTracers with the CPC was also better in the case of the higher concentration with deviations of the average concentrations between 1% and 18%.

The nanoCheck also shows an offset of 3120 #/cm^3, resulting in the instrument's better agreement with the CPC during NaCl-2 measurement (-9%) compared with NaCl-1 measurement ($+24\%$). Table 6 also gives the mean particle diameters measured by the different diffusion charger based devices as well as the geometric mean diameter calculated from the SMPS measurements. The average diameters, reported by the miniDiSCs are between 0.8% (miniDiSC-5) and 8.4% (miniDiSC-1) below the SMPS average diameter for NaCl-1 and between 5.9% and 16.9% below during NaCl-2 measurements. The mean particle sizes measured with the nanoTracers showed larger deviations between 24% (nanoTracer-4) and 33% (nanoTracer-1) with the lower NaCl particle concentration. With the higher concentration, the deviation decreased to 13% and 24%, respectively. The nanoCheck sizing agreed almost perfectly with the SMPS mean diameter during NaCl-1 measurement, and was approximately 9% below the SMPS value during NaCl-2.

The DEHS size distribution was expected to be a challenge for the diffusion charger based instruments, because the sizes of the DEHS particles towards the upper end of the size distribution exceed the nominal size ranges of the instruments. The modal diameter of the DEHS particles was around 250 nm with a tail reaching all the way up to approximately 1 μm (see Fig. 2). miniDiSC and nanoCheck are specified to measure accurately up to 300 nm only and the nanoTracer is limited to modal diameters of up to 120 nm (see Table 2). Asbach et al. (2012) recently found that at least the nanoTracer seemed to misinterpret the measured currents in a way that the reported number concentrations were up to a factor of 6.9 higher than the actual concentration, whereas the miniDiSC agreed to within a few percent. The nanoCheck showed on average about 23% higher concentrations, but the measured concentrations varied significantly, resulting in a lower correlation between the instrument and a CPC. The results summarized in Tables 5 and 6 agree well with these previous findings, except for a somewhat worse agreement between the miniDiSCs and the CPC. The average concentrations (Table 6) measured with the miniDiSC were up to 50% below those measured with the CPC. It should be noted here, however, that the DEHS particles used in the present study had a larger modal diameter (≈ 250 nm) than in the study by Asbach et al. (2012) (≈ 180 nm). Therefore there are more particles in the tail of the distribution that may distort the measurements. The mean particle sizes reported by miniDiSC-2 to miniDiSC-5 agreed better than the concentration with deviations between -14% and $+22\%$. Only miniDiSC-1 showed larger deviations of the mean particle size of around -30% for both DEHS-1 and DEHS-2. Interestingly miniDiSC-1 was the device that showed the lowest deviations of the concentrations and was the only miniDiSC that reported a higher concentration than the CPC. All miniDiSC concentrations were highly correlated with the CPC concentrations with $R^2 > 0.99$. Even though the nanoTracer concentrations were similarly well correlated with the CPC results, the agreement was poor. Concentrations reported by nanoTracer-3 were by a factor of 19 higher than those of the CPC. It was expected that this version of the nanoTracer must report much higher concentrations, because of the assumed particle diameter of 50 nm. If the particles are significantly

Table 6
Averages and standard deviations of mean diameters and number concentrations measured by the instruments and deviation from CPC number concentration and geometric mean diameter from SMPS measurement ; all diameters in [nm] and all concentrations in [#/cm^3].

Instrument ID		NaCl				DEHS				Soot					
		1		2		1		2		1		2		3	
miniDiSC-1	d_{mean} [nm]	37.44 ± 0.28	-8.4%	29.84 ± 0.16	−16.9%	184.30 ± 8.60	−30.2%	172.16 ± 6.40	−29.3%	80.19 ± 1.79	−24.5%				
	C_N [#/cm^3]	15,430 ± 287	5.0%	95,467 ± 3,180	0.9%	27,613 ± 1,583	20.9%	107,478 ± 5,025	7.2%	28,475 ± 944	21.3%	Failure		Failure	
miniDiSC-2	d_{mean} [nm]	39.91 ± 0.30	−2.3%	32.55 ± 0.17	−9.4%	243.77 ± 9.04	−7.6%	211.39 ± 5.12	−13.2%	90.79 ± 2.19	−14.5%	82.59 ± 1.12	−17.2%	47.85 ± 0.48	−18.3%
	C_N [#/cm^3]	14,225 ± 204	−3.2%	87,254 ± 2,896	−7.7%	15,472 ± 762	−32.3%	75,794 ± 2,795	−24.4%	25,687 ± 874	9.4%	85,793 ± 3,135	3.3%	89,791 ± 1,243	9.9%
miniDiSC-3	d_{mean} [nm]	40.76 ± 0.39	−0.3%	32.81 ± 0.16	−8.7%	293.88 ± 6.04	11.3%	250.79 ± 7.70	2.9%	103.52 ± 3.34	−2.5%	88.17 ± 1.76	−11.6%	48.79 ± 0.42	−16.7%
	C_N [#/cm^3]	14,585 ± 294	−0.8%	92,066 ± 3,232	−2.7%	10,502 ± 222	−54.0%	53,879 ± 1,918	−46.3%	22,084 ± 1,041	−5.9%	75,577 ± 3,652	−9.0%	90,257 ± 1,882	10.5%
miniDiSC-4	d_{mean} [nm]	40.42 ± 0.33	−1.1%	32.73 ± 0.18	−8.9%	290.41 ± 9.72	10.0%	234.85 ± 6.30	−3.6%	100.70 ± 3.18	−5.1%	88.03 ± 1.49	−11.7%	49.27 ± 0.48	−15.9%
	C_N [#/cm^3]	14,798 ± 262	0.7%	92,864 ± 3,370	−1.8%	11,876 ± 562	−48.0%	62,417 ± 2,396	−37.8%	23,764 ± 1,096	1.2%	87,987 ± 3,170	5.9%	92,501 ± 1,587	13.2%
miniDiSC-5	d_{mean} [nm]	40.56 ± 0.34	−0.8%	33.81 ± 0.17	−5.9%	299.93 ± 0.39	13.6%	298.80 ± 1.70	22.6%	104.74 ± 3.62	−1.3%	94.68 ± 1.8	−5.1%	49.69 ± 0.51	−15.2%
	C_N [#/cm^3]	14,183 ± 216	−3.5%	83,524 ± 3,027	−11.7%	11,759 ± 137	−48.5%	49,593 ± 602	−50.5%	21,663 ± 1,110	−7.7%	72,838 ± 2,973	−12.3%	84,910 ± 1,493	4.0%
nanoTracer-1	d_{mean} [nm]	54.17 ± 1.65	32.5%	44.50 ± 0.84	23.9%	Failure		Failure		Failure		93.28 ± 8.44	−6.5%	60.47 ± 1.99	3.2%
	C_N [#/cm^3]	16,605 ± 663	13.0%	95,487 ± 2,632	1.0%	250,047 ± 2,384	994.8%	942,115 ± 7,921	839.5%	77,494 ± 674	230.0%	129,203 ± 12,239	55.5%	98,910 ± 3,925	21.1%
nanoTracer-2	d_{mean} [nm]	Failure		Failure		216.15 ± 10.74	−18.1%	213.24 ± 11.79	−12.5%	101.51 ± 3.86	−4.4%	98.07 ± 3.74	−1.7%	57.17 ± 1.17	−2.4%
	C_N [#/cm^3]	17,682 ± 310	20.3%	77,363 ± 1,035	−18.2%	67,105 ± 3,621	193.8%	253,323 ± 14,697	152.6%	43,402 ± 1,938	84.8%	134,606 ± 5,445	62.0%	118,666 ± 3,006	45.3%
nanoTracer-3[a]	C_N [#/cm^3]	23,051 ± 366	56.9%	98,990 ± 1,029	4.7%	432,119 ± 4,462	1792%	1,524,011 ± 53,302	1420%	105,807 ± 1,034	350.6%	336,230 ± 15,209	304.7%	153,028 ± 5,228	87.3%
nanoTracer-4	d_{mean} [nm]	50.65 ± 1.35	23.9%	40.50 ± 0.70	12.7%							91.05 ± 2.75	−8.7%	55.85 ± 1.25	−4.7%
	C_N [#/cm^3]	18,950 ± 571	28.9%	109,999 ± 3,000	16.3%	Failure	Failure		Failure			145,952 ± 5,311	75.7%	123,417 ± 3,335	51.1%
nanoCheck	d_{mean} [nm]	40.70 ± 1.40	−0.4%	31.10 ± 0.35	−13.4%	168.98 ± 26.92	−36.0%	161.20 ± 29.84	−33.8%	71.90 ± 4.43	−32.3%	67.54 ± 2.04	−32.3%	39.45 ± 0.87	−32.7%
	C_N [#/cm^3]	18,163 ± 613	23.6%	86,292 ± 3,154	−8.8%	36,216 ± 7,335	58.6%	158,913 ± 38,642	58.5%	43,353 ± 3,554	84.6%	138,584 ± 6,168	66.8%	127,124 ± 3,447	55.6%
SMPS-G1	d_{geom} [nm]	40.87		35.93		263.95		243.67		106.15		99.75		58.6	
CPC	C_N [#/cm^3]	14,696 ± 129		94,582 ± 161		22,839 ± 161		100,282 ± 1,198		23,481 ± 787		83,091 ± 1,694		81,681 ± 919	

[a] Mean size assumed to be 50 nm.

Table 7
Average lung deposited surface area (alveolar) concentration, calculated from SMPS-G1 and measured with NSAMs and miniDiSCs.

Instrument ID LDSA [$\mu m^2/cm^3$]	NaCl				DEHS				Soot					
	1		2		1		2		1		2		3	
		Deviation[a]		Deviation[a]		Deviation[a]		Deviation[a]		Deviation[a]		Deviation[a]		Deviation[a]
SMPS-G1	**37.3**	−0.6%	**193.3**	2.6%	**590.6**	42.3%	**2324.9**	36.3%	**182.0**	2.5%	**590.2**	−7.9%	**319.5**	9.6%
NSAM-1	**37.5**		**188.4**		**414.9**		**1705.8**		**177.6**		**640.5**		**291.6**	
NSAM-2	**46.6**	24.2%	**222.6**	18.2%	**478.7**	15.4%	**1928.4**	13.0%	**201.0**	13.2%	**725.8**	13.3%	**331.8**	13.8%
miniDiSC-1	**29.9**	−20.2%	**142.3**	−24.5%	**337.7**	−18.6%	**1215.8**	−28.7%	**133.4**	−24.9%	Failure		Failure	
miniDiSC-2	**29.7**	−20.8%	**144.2**	−23.5%	**258.0**	−37.8%	**1073.6**	−37.1%	**138.0**	−22.3%	**412.9**	−35.5%	**231.2**	−20.7%
miniDiSC-3	**30.8**	−17.9%	**152.5**	−19.0%	**224.8**	−45.8%	**1045.1**	−38.7%	**138.8**	−21.9%	**405.3**	−36.7%	**239.1**	−18.0%
miniDiSC-4	**31.4**	−16.2%	**156.2**	−17.1%	**249.8**	−39.8%	**1124.7**	−34.1%	**145.8**	−17.9%	**444.3**	−30.6%	**251.7**	−13.7%
miniDiSC-5	**29.5**	−21.3%	**142.4**	−24.4%	**251.8**	−39.3%	**1165.4**	−31.7%	**135.6**	−23.7%	**417.7**	−34.8%	**227.5**	−22.0%

[a] Deviation from reference NSAM-1.

larger than this size, the extra current, which stems from the larger particles, is internally interpreted as a higher concentration. However, since the mean charge per particle scales approximately linearly with the particle diameter, a fivefold larger diameter should result in an approximately fivefold higher concentration. The reasons for the much larger increase remain unclear, but the same effect is also seen with the other nanoTracers in the test, which delivered between 2.5 and 11 times higher concentrations during DEHS measurements. The correlations between the nanoTracers and the CPC were slightly lower than those of the miniDiSCs, but can still be considered as good. Despite the relatively constant concentrations during the DEHS measurements, the nanoCheck showed strong fluctuations, as indicated by the large standard deviations of both the number concentration and the mean particle size in Table 6 as well as the low coefficient of determination $R^2=0.76$. On average, the nanoCheck concentrations were approximately 58% higher than the CPC concentrations and the mean particle sizes approximately 35% below those determined with SMPS-G1.

Measurements with soot particles revealed quite different reactions of the different instruments to agglomerated particles. The concentrations measured with the miniDiSCs showed agreement on the order of $\pm 20\%$ for all three experimental runs with soot particles. The deviations seem to be rather random and not clearly linked to the particle size or concentration. The sizing accuracy of the miniDiSC for soot particles is approximately in the same range. NanoTracer-3 again showed the highest deviations, with concentrations increased by a factor of 4.5 and 4 for soot-1 and soot-2 (both with a mean size of around 100 nm), respectively. The deviation was reduced to 87% for soot-3, when the mean particle size was 60 nm and hence closer to the size assumed by nanoTracer-3. nanoTracer-1 overestimated the particle number concentration by 230% in the case of soot-1 and 55% for soot-2. The regression analysis revealed a high offset of 38,700 #/cm^3. It is thus obvious that concentration levels of 24,000 #/cm^3 (soot-1) and 83,000 #/cm^3 (soot-2) cannot accurately be measured. In addition, the correlation between nanoTracer-1 and the CPC was rather poor with $R^2=0.81$. The agreement of the average concentration of nanoTracer-1 with the CPC for soot-3 was better (21% deviation), but the nanoTracer concentrations were still quite scattered, resulting in poor correlation ($R^2=0.83$). The agreement of nanoTracer-2 was quite similar, although the data showed better correlation. Unlike in the previous study (Asbach et al., 2012), the nanoCheck overestimated the number concentration by 85% and 67% in the case of soot-1 and soot-2 and by 56% in the case of soot-3. The mean diameters were all approximately 33% smaller than those obtained from SMPS-G1. This is not a contradiction to the previous study, because they used soot particles with a modal diameter of around 30 nm. Many particles were therefore likely deposited in the first stage of the nanoCheck that is designed to remove particles below approximately 25 nm. In the present study, soot particles were much larger and therefore not removed from the sample flow. Differences in the measured particle concentration may therefore be triggered by the particle shape. However, throughout the measurements in the present study, the nanoCheck reported higher concentrations and smaller mean diameters than the CPC and SMPS-G1, respectively. Although the deviations are higher for agglomerated soot particles than for the other two particle materials, this may only be seen as an indicator and require additional verification by simultaneous measurement with more than just one nanoCheck.

3.2.2. *Comparison of instruments measuring lung deposited surface area concentrations*

Table 7 gives an overview of the average alveolar LDSA concentrations from SMPS-G1, two NSAMs and the five miniDiSCs during each one hour experimental run and their deviations from the data calculated from SMPS-G1 assuming spherical particles. It can be seen that NSAM-1, which had been freshly calibrated, agreed well with SMPS-G1 for NaCl and soot particles. Similarly good agreement for small ammonium sulphate and TiO_2 particles (similar sizes like NaCl and soot particles in this study) between NSAM and SMPS has also been reported by Leskinen et al. (2012). The good agreement between SMPS-G1 and NSAM-1 for agglomerated soot particles also shows that the assumption of spherical particles in the calculation from SMPS data is justified, particularly since Fissan et al. (2012) hypothesized that differences between the true agglomerate surface area and the surface area of equivalent spheres are minute. For DEHS particles, SMPS-G1 LDSA concentrations were between 36% and 42% above NSAM-1. These higher deviations particles were not unexpected, because Asbach et al. (2009b) showed that the NSAM under-represents the LDSA concentrations for particles above approximately 300–400 nm, where the lung deposition curves show their minimum. DEHS particles above 300–400 nm contribute significantly to the surface area size distributions (compare with Fig. 2) and hence caused this deviation.

NSAM-2, which had not been calibrated before the study, showed between 13% and 24% higher concentrations than NSAM-1 for NaCl and soot and between 13% and 15% higher concentrations for DEHS. The results of NSAM-1 and NSAM-2 were highly correlated for all materials, with coefficients of regression $R^2 > 0.986$ as shown in Table 8. It was later found that the internal filters in NSAM-2 needed to be replaced. The clogged filters biased the flow rates and thus caused differences in the results. However, no error messages were received from the instrument, hence regular checks of an NSAM and its flow rates are recommended.

All miniDiSCs reported very similar results for all tested materials and concentrations. Deviations among miniDiSCs were all well within $\pm 10\%$ (except for miniDiSC-1 with DEHS). However, all miniDiSCs reported consistently lower LDSA concentration than NSAM-1. While for NaCl the deviation ranged from -16% to -25%, the deviation was between -19% and -46% with DEHS particles, showing that the miniDiSCs under-represent LDSA concentrations for DEHS even more strongly. The higher discrepancy with DEHS particles compared with NaCl particles are likely caused by the same reason as for the NSAM, i.e., the presence of particles larger than 300–400 nm. The results with soot particles revealed some interesting results. The agreement between all miniDiSCs and NSAM-1 was clearly lower for soot-2 than for soot-1, i.e., for

Table 8
Regression analyses for lung deposited surface area concentration (alveolar) with respect to NSAM-1; in the equations, y denotes the LDSA concentration of the respective instrument and x denotes the LDSA concentration of NSAM-1; all concentrations in ($\mu m^2/cm^3$).

Instrument ID	NaCl 1+2	DEHS 1+2	Soot 1+2	Soot 3
NSAM-2	$y=1.1808x+1.7885$ $R^2=0.9989$	$y=1.1483x+6.7104$ $R^2=0.9962$	$y=1.1288x+2.0460$ $R^2=0.9993$	$y=1.0821x+14.9376$ $R^2=0.9856$
miniDiSC-1	$y=0.7556x+2.9714$ $R^2=0.9936$	$y=0.7040x+34.9250$ $R^2=0.9966$	$y=0.7388x+1.8605$[a] $R^2=0.9448$	 Failure
miniDiSC-2	$y=0.7773x+2.0438$ $R^2=0.9898$	$y=0.6366x-4.3367$ $R^2=0.9966$	$y=0.6097x+23.3654$ $R^2=0.9942$	$y=0.5728x+65.8677$ $R^2=0.9384$
miniDiSC-3	$y=0.8171x+2.0438$ $R^2=0.9932$	$y=0.6360x-28.0745$ $R^2=0.9960$	$y=0.5920x+26.6300$ $R^2=0.9906$	$y=0.5573x+75.2720$ $R^2=0.9439$
miniDiSC-4	$y=0.8457x+1.2196$ $R^2=0.9935$	$y=0.6712x-19.6965$ $R^2=0.9973$	$y=0.6561x+24.0507$ $R^2=0.9939$	$y=0.6730x+55.0657$ $R^2=0.9750$
miniDiSC-5	$y=0.7679x+2.6495$ $R^2=0.9891$	$y=0.7002x-26.0749$ $R^2=0.9976$	$y=0.6182x+20.5246$ $R^2=0.9933$	$y=0.6753x+29.9042$ $R^2=0.9785$

[a] Soot-1 only.

the higher concentration, but otherwise nearly identical size distribution. Interestingly, the agreement for soot-3, i.e., similarly high concentration as for soot-2, but lower particle sizes, was even slightly better than for soot-1. This shows that the comparability of LDSA concentration measurements is no simple function of only particle size or concentration, but more likely a complex mixture of size, concentration and maybe morphology dependences.

All the results with soot aerosol were highly correlated with NSAM-1 data coefficients of determination $R^2 > 0.99$ (Table 8), except for soot-3 which showed slightly lower correlations.

4. Summary and conclusions

An intensive study on the comparability of aerosol measurement equipment for submicron particles has been conducted. Altogether 24 instruments were involved in the study, including eleven electrical mobility based devices for the measurement of particle number size distributions and 13 devices for the measurement of size-integrated number or lung deposited surface area concentrations. All instruments were simultaneously challenged with either sodium chloride (modal diameter 40 nm), DEHS (250 nm) or soot (100 nm or 60 nm) particles.

Among the mobility particle sizers, SMPSs showed the highest comparability. The sizing agreement was excellent for sodium chloride and soot particles with modal diameters between 40 nm and 100 nm. Observed deviations in the reported modal diameters were within a few percent for all SMPSs in the test, including Grimm as well as TSI instruments used with different settings, software versions and DMAs. For the larger (250 nm) DEHS particles, the sizing of Grimm and TSI SMPSs agreed very well with other SMPSs of the same manufacturer, but the modal diameters of the TSI instruments were on average around 15% larger than those reported by Grimm instruments with long-DMA. The size distributions delivered by one Grimm SMPS that was equipped with a short DMA consistently dropped significantly below the other size distributions for particle sizes >150 nm. The particle number concentrations reported by all SMPSs for the small (40 nm) sodium chloride particles agreed excellently with those from a UCPC with deviations on the order of only $\pm 5\%$, except for two Grimm SMPSs that still used an older version of the data acquisition and evaluation software. The concentrations provided by those two instruments were up to 40% higher than those from all other instruments. Similar deviations were observed throughout all measurements in the present study with these two devices, leading to the conclusion that the old software version significantly over-estimated the total particle number concentrations. In general the agreement of the number concentrations was not as good for the larger (250 nm) DEHS and agglomerated soot particles, where they deviated by around $\pm 25\%$ (except for the two SMPSs with old software that showed higher deviations). The reasons for the discrepancies are likely different for soot and DEHS. The test soot particles were elongated, agglomerated particles (see TEM images in Fig. 2). It has been reported that the charging efficiency of such particles deviates from the efficiency for spherical particles (Wen et al., 1984) which are assumed in the software of all SMPSs and therefore likely caused discrepancies. Differences during measurements with DEHS aerosol with a modal diameter of around 250 nm were possibly caused by the multiple charge correction of the SMPS data deconvolution.

The FMPSs in the study showed a lower comparability with the internal reference SMPS. One FMPS consistently deviated quite strongly and was hence considered as a faulty device. The other two FMPSs showed agreement with the SMPS roughly on the order of $\pm 25\%$ for the sizing and $\pm 30\%$ for the concentration. In general the agreement was best for compact NaCl particles with sizes around 40 nm and worse for larger DEHS and agglomerated soot particles. It was shown that the agreement was better for 60 nm than with 100 nm soot particles and concluded that the FMPS comparability is affected by both particle size as well as particle morphology.

Comparison of results from the size integrating concentration monitors showed that the expectable accuracy range is usually on the order of $\pm 30\%$ for mean particle size, number and LDSA concentration (in agreement with a previous study by Asbach et al., 2012). If the particle sizes are outside of the specified size range of the instruments, deviations can be

significantly higher than this. The nanoTracers reported DEHS (modal diameter around 250 nm) particle number concentrations that were up to a factor of about nine higher than concentrations measured with a CPC. One of the nanoTracers did not measure the particle size but assumed a constant particle diameter of 50 nm. This was shown to lead to highly inaccurate results if the actual particle sizes exceed this value. In the case of 250 nm DEHS particles, this nanoTracer reported concentrations that were too high by a factor of 14. miniDiSCs in the study mostly showed agreement within the specified accuracy range of $\pm 30\%$, unless the particles were too large as in the case of DEHS. For DEHS, the miniDiSC particle number concentrations were up to a factor of approximately two too low. This may have been caused by particle removal in the inlet impactor. Concentrations measured with Grimm nanoCheck were consistently 30–100% higher than CPC concentrations for all materials. The mean particle sizes measured by the monitors was generally found to be in satisfying agreement with those obtained from SMPS measurements for NaCl and soot aerosols with deviations on the order of $\pm 20\%$. For DEHS particles which at least in part exceeded the specified size range of the instruments, the comparability of the mean particle sizes was significantly lower.

LDSA concentration measurements revealed that results from a freshly calibrated NSAM agreed perfectly with those calculated based on data from SMPS-G1 for sodium chloride particles with 40 nm modal diameters. The agreement was still very good for soot particles with 60 nm and 100 nm modal sizes, respectively, when particles were assumed to be spherical for calculations from SMPS. This agrees well with the findings of Fissan et al. (2012). LDSA concentrations measured with all miniDiSCs were lower than those measured with NSAM and SMPS, but for NaCl and soot all within the specified accuracy range of $\pm 30\%$ (except for soot-3, which showed slightly higher deviations). LDSA measurements of DEHS particles all delivered significantly too low concentrations, because of significant surface area contributions of particles >300–400 nm, i.e., where the lung deposition curves show their minima. It has been reported before that NSAM cannot follow this change in the required response function (Asbach et al., 2009b). The present results suggest that the same holds true for LDSA measurements with miniDiSC.

In conclusion, the choice of an appropriate aerosol measurement instrument remains a compromise. The highest accuracy in the determination of particle size distributions can still be achieved with Scanning or Sequential Mobility Particle Sizers (SMPSs), but the instruments are slow and not able to deliver any meaningful results if the size distributions are quickly changing. Fast Mobility Particle Sizers provide a much higher time resolution and therefore also allow for the determination of fluctuating particle size distributions. The FMPS, however, trades in accuracy for time resolution. Monitors for the determination of size-integrated particle concentrations have the great advantage of being much easier to use and require a lot less effort for data evaluation. On the other hand the provided data set is limited to the respective concentration value and in some cases a mean particle size. According to Asbach et al. (2012), CPCs are still the most accurate means for determination of particle number concentration as they use a direct measurement principle but require a working liquid and are (with few exceptions) not portable. Diffusion charger based concentration monitors offer better portability, lower maintenance requirements and are usually battery operated. They are hence a preferred option for obtaining an exposure estimate e.g., in workplaces or as permanently installed monitors. Their comparability with CPCs is on the order of $\pm 30\%$.

Acknowledgements

This research was conducted under the umbrella of the nanoGEM project which is funded by the German Ministry for Education and Research (BMBF) under grant number 03X0105. The financial support is gratefully acknowledged.

References

Asbach, C., Fissan, H., Kaminski, H., Kuhlbusch, T.A.J., Pui, D.Y.H., Shin, H., Horn, H.G., & Hase, T. (2011). A low pressure drop pre-separator for elimination of particles larger 450 nm. *Aerosol & Air Quality Research*, *11*, 487–496.

Asbach, C., Kaminski, H., Fissan, H., Monz, C., Dahmann, D., Mülhopt, S., Paur, H.R., Kiesling, H.J., Herrmann, F., Voetz, M., & Kuhlbusch, T.A.J. (2009a). Comparison of four mobility particle sizers with different time resolution for stationary exposure measurements. *Journal of Nanoparticle Research*, *11*, 1593–1609.

Asbach, C., Fissan, H., Stahlmecke, B., Kuhlbusch, T.A.J., & Pui, D.Y.H. (2009b). Conceptual limitations and extensions of lung-deposited Nanoparticle Surface Area Monitor (NSAM). *Journal of Nanoparticle Research*, *11*, 101–109.

Asbach, C., Kaminski, H., von Barany, D., Kuhlbusch, T.A.J., Monz, C., Dziurowitz, N., Pelzer, J., Vossen, K., Berlin, K., Dietrich, S., Götz, U., Kiesling, H.J., Schierl, R., & Dahmann, D. (2012). Comparability of portable nanoparticle exposure monitors. *Annals of Occupational Hygiene*, *56*, 606–621.

Bau, S., Jacoby, J., & Witschger, O. (2012). Evaluation of the diffusion size classifier (meDiSC) for the real-time measurement of particle size and number concentration of nanoaerosols in the range 20–700 nm. *Journal of Environmental Monitoring*, *14*, 1014–1023.

Brouwer, D., van Duuren-Stuurman, B., Berges, M., Jankowska, E., Bard, D., & Mark, D. (2009). From workplace air measurement results towards estimates of exposure? Development of a strategy to assess exposure to manufactured nano-objects. *Journal of Nanoparticle Research*, *11*, 1867–1881.

Buzorius, G., Hämeri, K., Pekkanen, J., & Kulmala, M. (1999). Spatial variation of aerosol number concentration in Helsinki city. *Atmospheric Environment*, *33*, 553–565.

Cunningham, E. (1910). On the Velocity of Steady Fall of Spherical Particles through Fluid Medium. *Proceedings of the Royal Society Series A*, *83*, 357–365.

Dahmann, D. (1997). A novel test stand for the generation of diesel particulate matter. *Annals of Occupational Hygiene*, *41*(Suppl. 1), 43–48.

Dahmann, D., Riediger, G., Schletter, J., Wiedensohler, A., Carli, S., Graff, A., Grosser, M., Hojgr, M., Horn, H.G., Matter, U., Monz, C., Mosimann, T., Stein, H., Wehner, B., & Wieser, U. (2001). Intercomparison of mobility particle sizers (MPS). *Gefahrstoffe—Reinhaltung der Luft*, *61*, 423–427.

DIN EN 481 (1993) Workplaces atmospheres; size fraction definitions for measurement of airborne particles; German version.

Dixkens, J., & Fissan, H. (1999). Development of an electrostatic precipitator for off-line particle analysis. *Aerosol Science & Technology*, *30*, 438–453.

Duffin, R., Tran, C.L., Clouter, A., Brown, D.M., & MacNee, W. (2002). The importance of surface area and specific reactivity in the acute pulmonary inflammatory response to particles. *Annals of Occupational Hygiene*, *46*(Suppl. 1), 242–245.
European Parliament and the Council (2007). Regulation (EC) No 715/2007 on type approval of motor vehicles with respect to emissions from light passenger and commercial vehicles (Euro 5 and Euro 6) and on access to vehicle repair and maintenance information. *Official Journal of the European Union* June 2007, L171/1–L171/16.
Fierz, M., Houle, C., Steigmeier, P., & Burtscher, H. (2011). Design, calibration, and field performance of a miniature diffusion size classifier. *Aerosol Science & Technology*, *45*, 1–10.
Fissan, H., Asbach, C., Kaminski, H., & Kuhlbusch, T.A.J. (2012). Total surface area measurements of nanoparticles in gases with an electrical sensor. *Chemie Ingenieur Technik*, *84*, 365–372.
Fissan, H., Neumann, S., Trampe, A., Pui, D.Y.H., & Shin, W.G. (2007). Rationale and principle of an instrument measuring lung deposited nanoparticle surface area. *Journal of Nanoparticle Research*, *9*, 53–59.
Fissan, H., Helsper, C., & Thielen, H.J. (1983). Determination of particle size distribution by means of an electrostatic classifier. *Journal of Aerosol Science*, *14*, 354–357.
Fuchs, N.A. (1963). On the stationary charge distribution on aerosol particles in bipolar ionic atmosphere. *Geofisica Pura e Applicata*, *56*, 185–193.
Helsper, C., Horn, H.G., Schneider, F., Wehner, B., & Wiedensohler, A. (2008). Intercomparison of five mobility particle size spectrometers for measuring atmospheric submicrometer aerosol particles. *Gefahrstoffe—Reinhaltung der Luft*, *68*, 475–481.
Hinds, W.C. (1999). *Aerosol Technology—Properties, Behavior, and Measurement of Airborne Particles*. John Wiley & Sons, Inc.: New York.
Hoppel, W.A. (1978). Determination of the aerosol size distribution from the mobility distribution of the charged fraction of aerosols. *Journal of Aerosol Science*, *9*, 41–54.
ICRP (1994). *International Commission on Radiological Protection Publication 66 Human Respiratory Tract Model for Radiological Protection*. Elsevier Science Ltd.: Oxford, Pergamon.
Jeong, C.H., & Evans, G.J. (2009). Inter-comparison of a fast mobility particle sizer and a scanning mobility particle sizer incorporating an ultrafine water-based condensation particle counter. *Aerosol Science & Technology*, *43*, 364–373.
Jung, H., & Kittelson, D.B. (2005). Characterization of aerosol surface instruments in transition regime. *Aerosol Science & Technology*, *39*, 902–911.
Jung, H., Mulholland, G.W., Pui, D.Y.H., & Kim, J.H. (2012). Re-evaluation of the slip correction parameter of certified PSL spheres using a nanometer differential mobility analyzer (NDMA). *Journal of Aerosol Science*, *51*, 24–34.
Kaminski, H., Kuhlbusch, T.A.J., Fissan, H., Ravi, L., Horn, H.G., Han, H.S., Caldow, R., & Asbach, C. (2012). Mathematical description of experimentally determined charge distributions of a unipolar diffusion charger. *Aerosol Science & Technology*, *46*, 708–716.
Kim, J.H., Mulholland, G.W., Kuckuck, S.R., & Pui, D.Y.H. (2005). Slip correction measurements of certified PSL nanoparticles using a nanometer differential mobility analyzer (nano-DMA) for Knudsen number from 0.5 to 83. *Journal of Research of the National Institute of Standandards and Technology*, *110*, 31–54.
Koch, W., Pohlmann, G., & Schwarz, K. (2008). A reference number concentration generator for ultrafine aerosols based on Brownian coagulation. *Journal of Aerosol Science*, *39*, 150–155.
Kuhlbusch, T.A.J., John, A.C., & Fissan, H. (2001). Diurnal variations of particle characteristics at a rural measuring site close to the Ruhr area, Germany. *Atmospheric Environment*, *S35*, 13–21.
Kuhlbusch, T.A.J., Asbach, C., Fissan, H., Göhler, D., & Stintz, M. (2011). Nanoparticle exposure at nanotechnology workplaces: a review. *Particle and Fibre Toxicology*, *8*, 22.
Lall, A.A., & Friedlander, S.K. (2006). On-line measurement of ultrafine aggregate surface area and volume distributions by electrical mobility analysis: I. Theoretical analysis. *Journal of Aerosol Science*, *37*, 260–271.
Leskinen, J., Joutsensaari, J., Lyyränen, J., Koivisto, J., Russunen, J., Järvelä, M., Tuomi, T., Hämeri, K., Auvinen, A., & Jokiniemi, J. (2012). Comparison of nanoparticle measurement instruments for occupational health applications. *Journal of Nanoparticle Research*, *14*, 718.
Marra, J., Voetz, M., & Kiesling, H.J. (2010). Monitor for detecting and assessing exposure to airborne nanoparticles. *Journal of Nanoparticle Research*, *12*, 21–37.
Medved, A., Dorman, F., Kaufman, S.L., & Pöcher, A. (2000). A new corona-based charger for aerosol particles. *Journal of Aerosol Science*, *31*(S1), S616–S617.
Oberdörster, G. (2000). Toxicology of ultrafine particles: in vivo studies. *Philosophical Transactions of the Royal Society A*, *358*, 2719–2740.
Oberdörster, G. (2001). Pulmonary effects of inhaled ultrafine particles. *International Archives of Occupational and Environmental Health*, *74*, 1–8.
Oberdörster, G., Oberdörster, E., & Oberdörster, J. (2005). Nanotoxicology: an emerging discipline evolving from studies of ultrafine particles. *Environmental Health Perspectives*, *113*, 823–839.
Peters, A., Wichmann, H.E., Tuch, T., Heinrich, J., & Heyder, J. (1997). Respiratory effects are associated with the number of ultrafine particles. *American Journal of Respiratory and Critical Care Medicine*, *155*, 1376–1383.
Pui, D.Y.H., & Liu, B.Y.H. (1974). A submicron aerosol standard and the primary absolute calibration of the condensation nuclei counter. *Journal of Colloid and Interface Science*, *47*, 155–171.
Shi, J.P., Khan, A.A., & Harrison, R.M. (1999). Measurements of ultrafine particle concentration and size distribution in the urban atmosphere. *Science of the Total Environment*, *235*, 51–64.
Shin, W.G., Pui, D.Y.H., Fissan, H., Neumann, S., & Trampe, A. (2007). Calibration and numerical simulation of nanoparticle surface area monitor (TSI model 3550 NSAM). *Journal of Nanoparticle Research*, *9*, 61–69.
Tammet, H., Mirme, A., & Tamm, E. (2002). Electrical aerosol spectrometer of Tartu University. *Atmospheric Research*, *62*, 315–324.
Tran, C.L., Buchanan, D., Cullen, R.T., Searl, A., Jones, A.D., & Donaldson, K. (2000). Inhalation of poorly soluble particles. II. Influence of particle surface area on inflammation and clearance. *Inhalation Toxicology*, *12*, 1113–1126.
Wang, S.C., & Flagan, R.C. (1990). Scanning electrical mobility spectrometer. *Aerosol Science & Technology*, *13*, 230–240.
Watson, J.G., Chow, J.C., Sodeman, D.A., Lowenthal, D.H., Chang, M.C.O., Park, K., & Wang, X. (2011). Comparison of four scanning mobility particle sizers at the Fresno Supersite. *Particulology*, *9*, 204–209.
Wehner, B., Birmili, W., Gnauk, T., & Wiedensohler, A. (2002). Particle number size distributions in a street canyon and their transformation into the urban air background: measurements and a simple model study. *Atmosperic Environment*, *36*, 2215–2223.
Wen, H.Y., Reischl, G.P., & Kasper, G. (1984). Bipolar diffusion charging of fibrous aerosol particles—I. Charging theory. *Journal of Aerosol Science*, *15*, 89–101.
Wiedensohler, A. (1988). An approximation of the bipolar charge distribution for particles in the submicron size range. *Journal of Aerosol Science*, *19*, 387–389.
Winklmayr, W., Reischl, G.P., Lindner, A.O., & Berner, A. (1991). A new electromobility spectrometer for the measurement of aerosol size distributions in the size range from 1 to 1000 nm. *Journal of Aerosol Science*, *22*, 289–296.
Yli-Ojanpera, J., Mäkelä, J.M., Marjamäki, M., Rostedt, A., & Keskinen, J. (2010). Towards traceable particle number concentration standard: single charged aerosol reference (SCAR). *Journal of Aerosol Science*, *41*, 719–728.